Response to Reviewer # 1's Comments

Comment. 1 *The INSAT-3D is a new satellite and the basic datasets need to validated before CAPE calculation. So I suggest the authors to provide some analysis on how the INSAT temperature, humidity etc. performs over the Indian region, by comparing with radiosonde or reanalysis data. Since India has a large latitudinal extent from near equator in South to subtropics in the North, it is essential to investigate whether INSAT data compares well everywhere or there is some spatial inhomogeneity.*

Response **We agree with the referee's suggestion that the Indian region has a large latitudinal extent and spatial inhomogeneity can exists in the retrieval of the satellite data sets.**

Earlier studies by Mitra et al. (2015) and Ratnam et al. (2016) assessed the temperature and humidity retrievals from the INSAT-3D measurements using GPS sonde, reanalysis and other satellite measurements over the Indian region. They found a good agreement of INSAT-3D retrieved temperature with GPS sonde, reanalysis and satellite estimates below 25°N. The temperature difference was 0.5K with a standard deviation of about 1K, and for humidity, a dry bias (20-30%) was observed between INSAT-3D and GPS sonde data. This is already mentioned in the manuscript.

Comment. 2 *The authors need to highlight the advantages of their present study i.e. what new can we extract about CAPE by using the INSAT data. The authors mention in abstract that "In this work, an attempt is made for the first time to estimate CAPE from high spatial and temporal resolution measurements of the INSAT-3D over the Indian region". But there are many other satellites available back from many years and there are several studies related to CAPE over Indian region. So the authors need to discuss the why their work is important and how better it is from the previous estimates.*

Response **Several satellites measurements are available which can provide profiles of temperature and water vapour with reasonable accuracies. Most of them are polar orbiting satellites and have limited overpasses especially in the tropics. The other limitation of these polar satellite measurements is poor temporal resolution, even though they have global coverage.**

The significance of the INSAT-3D is its geostationary orbit, providing the profiles of temperature and water vapour with high temporal (1 hour) and spatial resolution ($0.1^{o} \times 0.1^{o}$) over the Indian and the surrounding oceanic regions. In the present study, the authors attempted to calculate CAPE from these high spatial and temporal resolution measurements of INSAT-3D and its performance assessment. To date there are no studies utilizing such high resolution data for such a long period to evaluate and understand the variability of CAPE. Hence, this study provides the direct usability of INSAT-3D data sets in the numerical weather prediction models for now-casting of thunderstorms and for severe weather conditions, which is lacking over the Indian region.

The relative sentence has been added in the revised manuscript.

Response to Reviewer # 2's Comments

General Comment	*This paper presents the temporal and spatial distribution of convective available potential energy (CAPE) estimated using INSAT-3D measurements. Initially, these CAPE estimates are compared with that estimated using ERA-Interim reanalysis and the radiosonde measurements obtained from 20 stations that are distributed across India. Statistical analysis has been made to get confidence on the estimated CAPE values. Finally, the diurnal and seasonal variability in the CAPE is also presented at different geographical locations.* *In general, paper is well written and contains significant original contribution. Authors have fully taken advantage of the high spatial and temporal measurements available from INSAT-3D to investigate the diurnal and season variability of CAPE. However, there are few mistakes and sometimes interpretation is missing at some instances without proper literature survey which demands careful editing or re-writing the sentences. Below are the some of the issues which authors need to take care before rendering judgment on the manuscript. Authors are strongly encouraged to revise and re-submit this manuscript.*
Response	**We are indebted to the reviewer for his valuable and thoughtful comments on the manuscript. We greatly appreciate the reviewer's time and efforts for evaluating the manuscript. We went through all the referee comments and suggestions and implemented the same in the revised manuscript. Point-to-point clarifications for referee's comments and how we have addressed each recommendation is given below.**
Comment 1	*There are few studies where global measurements of CAPE are available using GPS RO observations (Santhi et al., 2014). Since no observations are there to validate the CAPE at high spatial resolution, small analysis can be made how INSAT-3D estimated CAPE match with GPS RO measured CAPE, particularly over the ocean. Qualitative comparison can also be made.*
Response	**The GPS RO measurements are very sparse for a particular location and hence are statistically insignificant to compare GPS-RO CAPE with INSAT-3D CAPE. For instance, Santhi et al. (2014) observed a total number of 6 occultations in a month over $2^o \times 2^o$ grid around Gadanki, India. Among these occultation's, only 2 and 4 occultations reached below 0.5 km and 1 km respectively above the surface. When we looked into the number of occultation during the present study period over a particular station ($0.25^o \times 0.25^o$ grid), the total number of occultations are less than 40, which may not be statistically significant. Hence, the reviewer is requested to consider author's proposal for not including the GPS-RO measurements in the revised manuscript.**
Comment 2	*To the best of my knowledge, INSAT-3D data will not be available during the cloudy times. Since there are two monsoon seasons (SW and NE monsoon) over Indian region, huge data gaps are expected during these two seasons. While*

making composite analysis at both spatial and temporal scales, results are expected to be biased. How the authors have taken care this issue need to be discussed.

Response **We agree with the reviewer. However, for the present analysis we have taken only cloud free conditions. The confidence level for the identification of the cloud free region is based on the cloud flag which is set to zero (CLD_FLG=0).**

The total number of data for the 20 stations considered in the study during different seasons is provided in Table 1. Since the INSAT-3D data are available for every one hour, the data gaps are not huge during both the monsoon seasons.

The relative sentences and Table are added in the revised manuscript.

Table 1: The total number of data available in 20 stations during different seasons for the period from April 2014 to March 2017.

Station	**Latitude**	**Longitude**	**Total Number of Data**			
			Winter	**Pre-monsoon**	**Monsoon**	**Post-monsoon**
Agarthala (AGR)	23.88	91.25	3614	3272	2615	2613
Ahmedabad (AHB)	23.06	72.63	3808	4034	3686	2891
Amini Divi (AMD)	11.12	72.73	3985	3776	3327	2362
Bhuvaneswar (BHU)	20.25	85.83	3701	3450	2389	2488
Chennai (CHE)	13.00	80.18	3816	3712	2956	1985
Cochin (COC)	9.95	76.26	3867	3072	2905	1758
Delhi (DEL)	28.58	77.20	2910	3316	3845	2894
Dibrugarh (DIB)	27.48	95.01	3287	2260	2536	2595
Gorakhpur (GRK)	26.75	83.36	2871	3383	2769	2833
Guwahati (GUW)	26.10	91.58	3610	3058	2956	2796
Hyderabad (HYD)	17.45	78.46	2550	394	327	1045
Karaikal (KAR)	10.91	79.83	3660	3458	3632	1846
Kolkata (KOL)	22.65	88.45	3488	2924	2500	2677
Machilipatnam (MAP)	16.20	81.15	4001	3706	2564	2322

Mangalore (MAN)	12.95	74.83	4063	3542	2705	2232
Minicoy (MIN)	8.30	73.15	3882	3346	3320	2040
Mumbai (MUM)	19.11	72.85	4294	4321	3405	2756
Port Blair (PB)	11.66	92.71	3676	3458	2381	2178
Trivandrum (TVM)	8.48	76.95	3675	3116	3608	1805
Visakhapatnam (VSP)	17.70	83.30	3972	3747	2632	2415

Comment 3 *It is mentioned (Line 101) that 'They observed that the INSAT-3D measurements compare better with GPS sonde observations at middle levels (from 900 hPa to 500 hPa).'. In this case how it is going to affect the estimates of CAPE need to be discussed. Further, how large bias observed in water vapor measurements from INSAT-3D is going to affect the CAPE estimates need to be discussed in detail.*

Response **CAPE is associated with the changes in the temperature and moisture in the troposphere. However, the changes in CAPE are more related to the moisture present in the boundary layer. Zhang (2002) showed that the net changes in the CAPE come from the thermodynamic changes in the boundary layer. They also showed that the changes in CAPE due to the changes in the temperature and moisture in the free troposphere is about 10% or less when compared to changes in temperature and moisture in the boundary layer. Hence, the changes in the INSAT-3D measurements at the lower levels affect much the changes in the CAPE compared to the changes in the middle levels.**

The error in estimating the CAPE is determined by applying the standard error propagation formula (Bevington and Robinson, 1992). The error in the CAPE calculation depends on the temperature and water vapour retrievals. In this study, an error of 5% in the measured relative humidity and temperature corresponds to an error of 8% in the calculated CAPE from the INSAT-3D measurements.

Comment 4 *Do authors have any explanation why there is a consistent positive (negative) bias (most of the cases) in CAPE values measured by INSAT-3D (ERA-Interim)?*

Response **The exact reason is very difficult to be pointed out. However, the reanalysis in general is an assimilated output with prior assumptions. The meteorological parameters of the reanalysis are always underestimated with respect to the observations. For example, Ratnam et al. (2013) have shown the comparison of humidity obtained from SAPHIR–A megha tropiques payload with respect to all reanalysis over the tropics. The humidity was underestimated in reanalysis. This may be the reason for the**

negative bias in the reanalysis. Radiosonde and INSAT-3D being both observations shows a positive bias.

Comment 5 *Do authors have any explanation why no variation is seen for large spatial gird in Fig.6 during pre-monsoon?*

Response **In India, the pre-monsoon season is most favourable for the development of thunderstorms over land regions. The surrounding oceanic regions have frequent development of depressions and these depressions sustained over oceanic region for few days. This results in higher values of CAPE over a large spatial extent for few days. This is the reason why no variation in CAPE is observed over large spatial grid during pre-monsoon season.**

Comment 6 *Introduction is too long without focus. It can be cut to 50% while retaining only relevant information. Diurnal and high spatial resolution studies only need to be highlighted.*

Response **As per the referee's suggestion, the introduction section has been modified in the revised manuscript.**

Minor Comments

Comment 1 *Line 142: It is mentioned that radiosonde data has been taken from University of Wyoming website. Note that this is not the quality checked data. Instead, it will be better to use data from IGRA2.*

Response **We appreciate the referee for his suggestion.**

The analysis is performed with IGRA2 dataset for the 20 stations considered in the study. As an example, the scatter plot between INSAT-CAPE and IGRA2-CAPE is shown in fig. 1. Even in the case of IGRA2 data also, the INSAT derived CAPE shows good correlation with a correlation coefficient of 0.72.

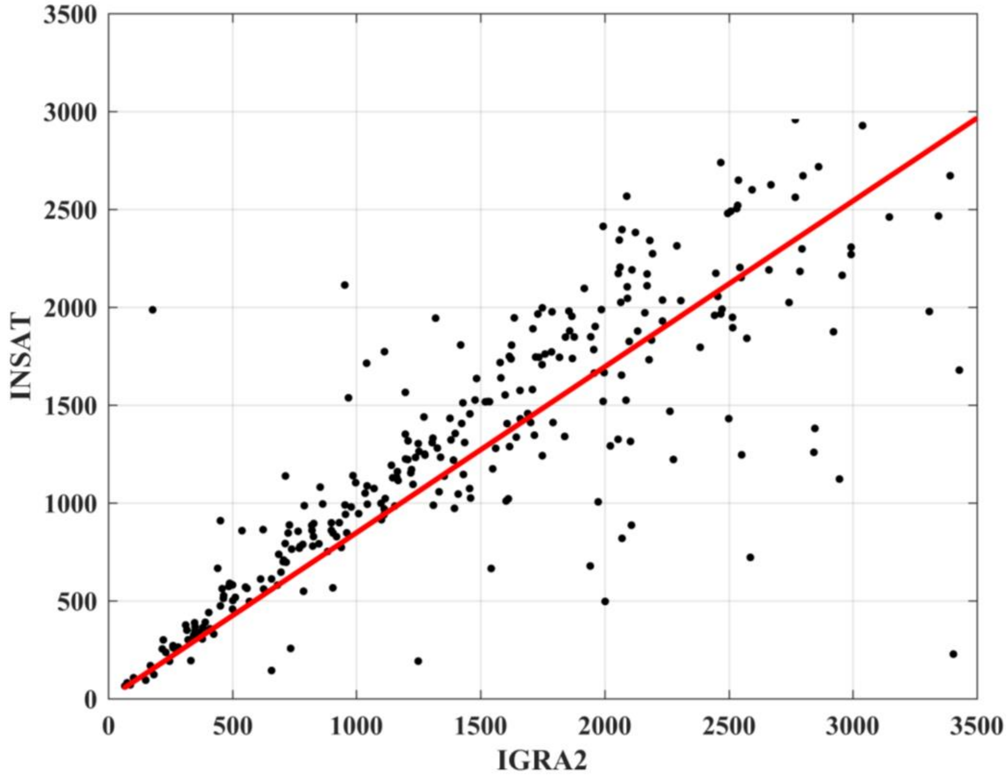

Fig. 1: Scatter plot between IGRA2 derived CAPE (J kg^{-1}) and INSAT derived CAPE (J kg^{-1}) for Chennai during April 2014 to March 2017.

Similarly, the correlation coefficient for CAPE derived from IGRA2 dataset and INSAT-3D data is provided for the reviewer in table 2. The INSAT-3D derived CAPE shows better correlation for most of the stations considered in the study. This shows the consistency of the INSAT-3D derived CAPE over IGRA2 dataset.

Table.2: ***Correlation coefficient in the comparison of INSAT-3D CAPE with IGRA2 and Wyoming derived CAPE for 20 stations in India for the period from April 2014 to March 2017.***

Station	*IGRA2*	*Radiosonde*
AGR	0.61	0.62
AHB	0.56	0.38
AMD	0.48	0.46
BHU	0.59	0.62
CHE	0.72	0.84

COC	0.50	0.81
DEL	0.65	0.31
DIB	0.72	0.44
GRK	0.64	0.46
GUW	0.72	0.59
HYD	0.51	0.59
KAR	0.73	0.56
KOL	0.57	0.55
MAP	0.57	0.62
MAN	0.42	0.68
MIN	0.56	0.64
MUM	0.43	0.64
PB	0.40	0.48
TVM	0.71	0.52
VSP	0.55	0.68

It can be observed from the above table that the correlation coefficient in the comparison of INSAT-3D CAPE with IGRA2 and radiosonde CAPE are almost similar for most of the stations. Hence, the inclusion of IGRA2 data in the manuscript is not going to affect the results of the study. So, the reviewer is requested to consider the use of Wyoming university data in the manuscript.

Comment 2 *Line 155: It was mentioned that the resolution of the data utilized is 0.75^o_0.75^o from ERA-Interim and 0.25^oX0.25^o from INSAT-3D. How this different spatial resolutions grids are taken care while comparing the CAPE estimates.*

Response **The authors apologize for the typographical error. For the present study, the authors make use of the ERA-Interim data at $0.25^o \times 0.25^o$ spatial resolution.**
The relative sentence is modified in the manuscript.

Comment 3 *Line 282: It is mentioned that 'The estimated CAPE is divided into four categories: weak instability (<500 J kg-1), moderate instability (501-1500 J kg-1), strong instability (1501-3000 J kg-1), and extreme instability (>3000 J kg-1).' Do you have any scientific justification to choose these thresholds? You may provide suitable reference.*

Response **These CAPE ranges are considered arbitrarily.**

Comment 4 *Line 338: It is mentioned that 'These regions are: the Arabian Sea (AS; 8-20oN, 65-72oE), Bay of Bengal (BoB; 8-20oN, 80-90oE), South Peninsular India (SP; 8-20oN, 72-80oE), Central India (CI; 20-25oN, 73-82oE), North India (NI; 25-35oN, 73-80oE), and Northeast India (NE; 24-29o34o N, 90-96oE).' Is there any scientific justification to choose these latitude longitude grids? You may provide suitable reference.*

Response **To understand the diurnal variation of CAPE over different parts of India, the study region is divided (latitude-wise for uniformity) into six sub-regions; Arabian Sea (AS; 8-20^{o}N, 65-72^{o}E), Bay of Bengal (BoB; 8-20^{o}N, 80-90^{o}E), South Peninsular India (SP; 8-20^{o}N, 72-80^{o}E), Central India (CI; 20-25^{o}N, 73-82^{o}E), North India (NI; 25-35^{o}N, 73-80^{o}E), and Northeast India (NE; 24-29^{o}N, 90-96^{o}E) as given in Raut et al. (2009).**
The relative reference is added in the text in the revised manuscript.

Comment 5 *Line 411: It is mentioned that several interesting features are noticed. 'The weak instability is predominant during the winter season, the moderate instability is higher during the post-monsoon, the strong instability is more during the monsoon period and the extreme instability is higher during the pre-monsoon months.' Note that these things are well known to the scientific community.*

Response **The above sentence is re-written as "The spatial and temporal distribution of CAPE reveals that the weak instability is predominant during winter season, moderate instability is higher during post-monsoon, strong instability is more during monsoon period and extreme instability is higher during pre-monsoon months".**

Comment 6 *It seems INSAT-3DR is being launched as a follow up of INSAT-3D. Did you tested how CAPE behaves between these two instruments?*

Response **INSAT-3DR is a redundancy payload for INSAT-3D and hence we have not attempted to calculate CAPE with INSAT-3DR data. In future, this will be our follow-up study.**

Comment 7 *Figure 1 caption: It is better to shift the latitude and longitude along with the name of the station to the running text rather keeping lengthy figure caption.*

Response **Referee's suggestion is implemented in the manuscript.**

Comment 8 *Figure 8: There are white patches over Tibetan high and also over the central India in few panels. Hope the reasons for the data gaps at these two places is not the same?*

Response **The white patches in the Tibetan high are due to the non-availability of data due to topography. Over Central India, it is mostly due to non-availability of data.**

Refrences:

Venkat Ratnam, M., Basha, G., Krishna Murthy, B. V., & Jayaraman, A. (2013). Relative humidity distribution from SAPHIR experiment on board Megha-Tropiques satellite mission: Comparison with global radiosonde and other satellite and reanalysis datasets, *Journal of Geophysical Research Atmospheres*, 18, 1–9, doi:10.1002/jgrd.50699.

Raut, B. A., Karekar, R. N., & Puranik, D. M. (2009). Spatial distribution and diurnal variation of cumuliform clouds during Indian Summer Monsoon. *Journal of Geophysical Research Atmospheres*, *114*(11), 1–12. https://doi.org/10.1029/2008JD011153

Santhi, Y. D., Ratnam, M. V., Dhaka, S. K., & Rao, S. V. (2014). Global morphology of convection indices observed using COSMIC GPS RO satellite measurements. *Atmospheric Research*, *137*, 205–215. https://doi.org/10.1016/j.atmosres.2013.10.002

Zhang, G. J. (2002). Convective quasi-equilibrium in midlatitude continental environment and its effect on convective parameterization. *Journal of Geophysical Research Atmospheres*, *107*(14), 1–16. https://doi.org/10.1029/2001JD001005

Retrieval of convective available potential energy from INSAT-3D measurements: comparison with radiosonde data and its spatial-temporal variations

Uriya Veerendra Murali Krishna[1], *Subrata Kumar Das*[1*], *Kizhathur Narasimhan~~K. N.~~ Uma*[2], *and G~~.~~ ovindan Pandithurai*[1]

[1]Indian Institute of Tropical Meteorology, Pune-411008, India

[2] Space Physics Laboratory, Vikram Sarabhai Space Centre, Trivandrum-695022, India

[*]Correspondence to Subrata Kumar Das (skd_ncu@yahoo.com)

Abstract:

Convective available potential energy (CAPE) is a measure of the amount of energy available for convection in the atmosphere. The satellite-derived data over the ocean and land is used for a better understanding of the atmospheric stability indices. In this work, an attempt is made for the first time to estimate CAPE from high spatial and temporal resolution measurements of the INSAT-3D over the Indian region. The estimated CAPE from the INSAT-3D is comprehensively evaluated using radiosonde derived CAPE and ERA-Interim CAPE. The evaluation shows that the INSAT-3D CAPE reasonably correlated with the radiosonde derived CAPE; however, the magnitude of CAPE shows higher values. Further, the distribution of CAPE is studied for different instability conditions (different range of CAPE values) during different seasons over the Indian region. In addition, the diurnal and seasonal variability in CAPE is also investigated at different geographical locations to understand the spatial variability with respect to different terrains.

Keywords: CAPE; Diurnal; INSAT-3D; ~~Monsoon; Diurnal;~~ Instability; -Monsoon

1. Introduction

The interaction between convection, clouds radiation, and large-scale circulation remains a major source of uncertainty in understanding the climate and climate change. Convection plays a crucial role in the formation of clouds (cumulonimbus). The convective activity prevailing over the atmosphere is the feeding mechanism for the development of weather systems such as thunderstorms and cyclones. Deep convection is one of the usual phenomena in the tropical region which requires three ingredients: instability, moisture, and uplift. Convective available potential energy (CAPE; Moncrieff and Miller, 1976) is a measure of convective potential in the atmosphere that incorporates the instability and moisture ingredients (Johns and Doswell, 1992). In a physical sense, it is the energy available for the free lifting of the air parcel from the level of free convection to the level of neutral buoyancy. CAPE is also the measure of maximum kinetic energy per unit mass of air parcel achievable by convection of moist air (Murugavel et al., 2012). So it can also be used as an estimator of maximum possible updraft velocity.

Climatology of CAPE provides valuable information for severe weather forecasting. Comparing this climatology to near real-time observations from meteorological sensors on satellites could provide valuable information in assessing the risk of severe weather (Breznitz 1984; Golden and Adams 2000; Doswell 2004; Barnes et al., 2007; Rothfusz et al., 2014; Cintineo et al., 2014). For example, high value of CAPE is an indicator of deep convection (Bhat et al., 1996). Johns and Doswell (1992) showed that the largest hail sizes in convection are related to CAPE. In severe weather conditions, CAPE is one of the key indices determining the occurrence of thunderstorms and tornadoes (McNulty, 1995). Further, Williams and Renno (1993) and Dutta and De (1999) have shown that the isolated heavy rainfall events on any isolated day result from a higher value of CAPE. Craven (2000) found that higher CAPE values and steep lapse rates were ideal for supercell storm and tornado

Formatted: Adjust space between Latin and Asian text, Adjust space between Asian text and numbers formation. Williams et al. (2002) suggested that CAPE can be used as a predictor of electrification/lightning intensity in deep tropical convection. The changes in convective activity and atmospheric energy budget are associated with the long-term changes in CAPE (Gettelman et al., 2002; DeMott and Randall, 2004; Riemann-Campe et al., 2008; Brooks, 2013). Hence, CAPE can also be used as a potential indicator of climate change (Gettelman et al., 2002; DeMott and Randall, 2004; Riemann Campe et al., 2008; Murugavel et al., 2012; Brooks, 2013). Thus, the behaviour of convection can be partially addressed by understanding the changes in CAPE.

Variability in CAPE can also affect the temperature field in the upper troposphere (Gaffen et al., 1991; Dhaka et al., 2010). Gaffen et al. (1991) discussed the dynamical link between lower tropospheric CAPE and variations in the temperature in the upper troposphere. For example, Dhaka et al. (2010) studied the relationship between seasonal, annual, and large-scale variations in CAPE and the solar cycle on the temperature at 100 hPa pressure levels using daily radiosonde data for the period 1980–2006 over the Indian region. They showed that the increase in CAPE was associated with the decrease in temperature at 100-hPa pressure level on all time scales.

The convective schemes in general circulation models use CAPE as a variable for calculating convective heating (e.g., Arakawa and Schubert, 1974; Moncrieff and Miller, 1976; Washington and Parkinson, 2005; Lee et al., 2007). Many of the cumulus parameterization schemes make use of CAPE in constructing closures (Donner and Phillips, 2003). The diurnal variation of CAPE is of primary importance for understanding the sensitivity of convection schemes in the model to produce the diurnal cycle of precipitation (Lee et al., 2007). The reliability of model-simulated temporal and spatial variations in CAPE is an important indicator of model performance, particularly in the tropics (Gettelman et al., 2002). Also, the seasonal and diurnal changes in CAPE are important for models to provide

Formatted: Indent: First line: 0 cm, Adjust space between Latin and Asian text, Adjust space between Asian text and numbers

Formatted: Adjust space between Latin and Asian text, Adjust space between Asian text and numbers validation of their capacity to simulate future changes in the tropical climate. The above studies conclude that the estimation of CAPE ~~are~~is imperative, not only for assessing the conditional instability of the atmosphere and for the convective parameterization, but also for the studies related to climatic change.

Most of the earlier studies on CAPE are based on radiosonde observations. Globally, the radiosonde is launched twice a day, 0000 and 1200 UTC. This limits the studies on CAPE at diurnal scales. It is also to be noted that the radiosonde observations are limited to land, and are very sparse over the oceans. Reanalysis datasets fill these gaps; however, their spatial resolution is poor and most of the time the data accuracies do not match with the standard techniques. The satellite observations are the only solutions to have regular observations of CAPE with high spatial resolution across the globe. With the availability of satellite measurements, several studies were carried out on CAPE. Narendra Babu et al. (2010) studied the seasonal and diurnal variations in CAPE over land and oceanic regions using one year of observations from the FORMOSAT mission 3/Constellation Observing System for Meteorology, Ionosphere, and Climate (COSMIC/FORMOSAT-3) Global Positioning System (GPS) Radio Occultation (~~GPS -~~GPS-RO) measurements. Santhi et al. (2014) estimated various stability indices using COSMIC GPS~~-~~-RO profiles and the uncertainty in estimating these stability indices. They also studied the diurnal variation of these stability indices over Gadanki, India. In order to study the diurnal variation of stability indices, they integrated the data over a season as the occultations were sparse and hence not adequate to study on daily scale. This limitation of under sampling can be overcome by the use of geostationary satellites. These geostationary satellite measurements provide near-continuous monitoring of ~~instability in~~ the atmosphere with better spatial coverage, which is helpful in nowcasting of convection (Koenig and de Coning, 2009). Siewert et al. (2010) discussed the advantages of the METEOSAT Second Generation (MSG) system in deriving the instability indices and to predict the convection initiation over the Central Europe and South Africa. Using the MSG satellite measurements, de Coning et al. (2011) derived a new convection indicator, the combined instability index which can calculate the probability of convection over the South Africa. They showed that the combined instability index can predict the convection better than the individual instability indices like K-index, total totals index etc. Jewett and Mecikalski (2010) developed an algorithm to derive convective momentum fluxes from the Geostationary Operational Environmental Satellite (GOES) measurements. The advantage of this algorithm is that it can be used in any convective environment. ~~Botes et al. (2012) investigated the performance of the Atmospheric Infrared Sounder (AIRS) soundings data with the collocated radiosonde observations. They showed that the AIRS measurements underestimate instability due to dry bias at the surface.~~

Recently, the Indian Space Research Organization (ISRO) launched the Indian National Satellite System (INSAT-3D), which is a geostationary satellite that provides the profile of temperature and relative humidity with high temporal and spatial resolution. ~~The purpose of the INSAT-3D measurement is to enhance the understanding of the atmospheric processes and also to monitor land and oceans in order to accurately forecast weather and to manage disasters.~~ Several researchers evaluated the temperature and relative humidity measurements from the INSAT-3D. Mitra et al. (2015) evaluated the INSAT-3D temperature and moisture retrievals up to 100 hPa with GPS sonde observations for the period January-May 2014. They observed that the INSAT-3D measurements compare better with GPS sonde observations at middle levels (from 900 hPa to 500 hPa). The assessment of the quality of temperature and water vapour obtained from the INSAT-3D with in-situ, satellite, and reanalysis datasets by Ratnam et al. (2016) revealed that the INSAT-3D measurements agree well with the GPS sonde observations, ~~other~~ satellite measurements and reanalysis datasets below 25^{o}N. The temperature difference was 0.5K with a standard deviation of about 1K, and for humidity, a dry bias (20-30%) was observed between INSAT-3D and GPS sonde observations~~other satellite measurements and reanalysis data~~. Hence, these satellite measurements also suffer from some inherent shortcomings and have biases and random errors. Therefore, it is essential to evaluate the satellite products with conventional measurements to quantify the direct usability of these products.

The objective of the present study is to calculate CAPE from high spatial and temporal resolution measurements of INSAT-3D over the Indian region and its performance assessment. To date there are no studies utilizing such high-resolution data for such a long period to evaluate and understand the variability of CAPE. Hence, this study provides the direct usability of INSAT-3D data sets in the numerical weather prediction models for nowcasting of thunderstorms and for severe weather conditions, which is lacking over the Indian region. In this work, we first attempted to ~~The objective of the present study is to quantitatively evaluate the accuracy of CAPE estimated from the INSAT-3D measurements with radiosonde measurements over the Indian region. Here, an attempt is made first to~~ validate the estimated CAPE from the INSAT-3D measurements with that of radiosonde measurements over different stations in India. In general, there are many profiles that do not reach the ground level in the INSAT-3D measurements. Hence, different statistical indices are calculated to assess the detectability of INSAT-3D derived CAPE over these regions. Secondly, the diurnal variation of CAPE is studied at different regions in India. Finally, the seasonal mean CAPE is estimated over the Indian region. The paper is organized as follows. Section 2 provides the details of the data sets used. Section 3 discusses the methodology adopted to estimate the CAPE. Section 4 provides the results and discussion. Finally, ~~the~~ summary of the present study is provided in section 5.

2. Database

2.1. *INSAT-3D*

In the present study, three years (01 April 2014 - 31 March 2017) of measurements obtained from the INSAT-3D are used to estimate CAPE over the Indian region and assess the estimation against radiosonde measurements. The INSAT is a series of multipurpose geostationary satellites launched by the ISRO, India. The INSAT-3D, which is considered to be the advanced version of all the other INSAT series satellites, is a multipurpose geosynchronous spacecraft with main meteorological payloads (imager and sounder) launched on 26 July 2013. The main objective of the mission is to monitor the earth and ocean continuously and also provide data dissemination capabilities. The INSAT-3D also provides an operational, environmental and storm warning system to protect life and property.

The INSAT-3D spacecraft carries two meteorological payloads: (i) Imager (optical radiometer) provides high-resolution images of mesoscale phenomena in the visible and infrared (IR) spectral bands (0.55 to 12.5 µm) and (ii) Sounder has one visible and 18 IR (7 in long-wave IR, 5 in mid-IR, and 6 in short-wave IR) channels. The sounder measures the irradiance and provide profiles of temperature, water vapour and integrated ozone over the Indian landmass and surrounding ocean every hour and over the whole of the Indian Ocean every 6 hours with a spatial resolution of 0.1^o. ~~This is the simplest scanning mode in which the soundings are available every hour over larger land and ocean region.~~ For the present study, temperature and water vapour data collected from the INSAT-3D sounder during the clear (cloud free) conditions. These dataset are interpolated to 0.25^o spatial resolution and are used to estimate the CAPE over the Indian region.

2.2. *Radiosonde*

Upper air radiosonde profiles are downloaded from the University of Wyoming website (http://weather.uwyo.edu/upperair/sounding.html). Radiosonde data are usually available at 0000 and 1200 UTC regularly to monitor the thermodynamic state of the atmosphere by the National Weather Service. For the present study, the data collected for 20 stations (black dots in Fig.ure 1) for the period from 01 April 2014 to 31 March 2017 are used to assess the INSAT-3D estimated CAPE. The values of CAPE reported in this paper are taken directly from the data provided by the University of Wyoming.

2.3. *ERA-Interim Reanalysis*

The reanalysis dataset used in this study are from the ERA-Interim project (Dee et al., 2011). The ERA-Interim is the latest global atmospheric reanalysis produced by the European Centre for Medium-Range Weather Forecasts (ECMWF), which envisaged preparing a future reanalysis project that will span the entire twentieth century. The ERA-Interim data are available in near-real time from 1 January 1979 onwards. The ERA-Interim generates gridded data, including a large variety of surface parameters that describe the weather as well as land surface and ocean conditions at the 3-hourly and 6-hourly interval. The present study utilizes the CAPE derived from the ERA-Interim dataset. The data are extracted over the Indian region at 0000, 0300, 0600, 0900, 1200, 1500, 1800 and 2100 1200 UTC for each day between 01 April 2014 and 31 March 2017. The spatial resolution of the data utilized is $0.75^o \times 0.75^o$ $0.25^o \times 0.25^o$.

3. Estimation of CAPE

To calculate the CAPE over the Indian region, the vertical profiles of pressure, temperature, and water vapour are taken from the INSAT-3D measurements. For many years, a debate has existed in the literature regarding the most meaningful way to calculate CAPE and how to interpret the result. The most important methods of calculating CAPE is (1) pseudoadiabatic CAPE in which CAPE is estimated after assuming that all the condensate has fallen out of the air parcel and (2) reversible CAPE in which it is assumed that the condensate remains within the parcel. In the present study, the pseudoadiabatic algorithm is used to calculate CAPE ~~over the Indian region~~. Further, CAPE is very sensitive to near-surface temperature and humidity (Gartzke et al., 2017), which are known to vary spatially. However, Ratnam et al. (2016) found that the variability of the atmospheric state within the INSAT-3D footprint sampled by the radiosonde had little bias over the Indian region. They also reported that the difference in temperature between INSAT-3D and ERA-Interim reanalysis datasets lies within 1K and a dry bias of 5–10% was found in the lower and mid-troposphere relative humidity when compared with the ERA-Interim reanalysis datasets. In this scenario, it is assumed that the spatial sampling mismatch may not affect much in the calculation of CAPE and hence are neglected in the present study. In addition, only cases with radiosonde profiles having CAPE greater than 0 J kg^{-1} are included in the analysis. This threshold is used to eliminate the large number of zero CAPE values.

The integration of the buoyancy of the air parcel from the level of free convection (LFC) to equilibrium level (EL) gives the measure of CAPE.

$$CAPE = \int_{LFC}^{EL} \frac{g(T_{vp} - T_{ve})}{T_{ve}} dZ \qquad (1)$$

Where, T_{vp} is the virtual temperature of the air parcel and T_{ve} is the virtual temperature of the environment, g is the acceleration due to gravity. The LFC is situated above the lifting condensation level (LCL) and at that level, the parcel temperature is greater than the environmental temperature. This is calculated by lifting the air parcel moist adiabatically. The EL is situated above the LFC and at this level, the parcel temperature is less than or equal to the environment temperature. At EL, the air parcel attains stability and the convection stops. Under stable environmental conditions, the LFC and EL will not be present. The procedure to estimate CAPE is similar as discussed in Uma and Das (2017).

Formatted: Font: Italic

The error in estimating the CAPE is determined by applying the standard error propagation formula (Bevington and Robinson, 1992). The error in the CAPE calculation depends on the temperature and water vapour retrievals. In this study, an error of 5% in the measured relative humidity and temperature corresponds to an error of 8% in the calculated CAPE from the INSAT-3D measurements.

Formatted: Indent: First line: 1.27 cm

4. Results and Discussions

Three years of data collected from the INSAT-3D measurements are utilized to estimate CAPE over the Indian region. These estimates are compared with the radiosonde derived CAPE at 0000 and 1200 UTC along with the ERA-Interim reanalysis CAPE data.

4.1. *Comparison of INSAT-3D CAPE with radiosonde and ERA-Interim ~~estimated~~ CAPE ~~with radiosonde measurements~~*

In this work, 20 stations are selected for which the radiosonde profiles are available during the study period (location shown in Fig. 1). Table 1 provide the details of the stations considered along with the total number of data available from INSAT-3D measurements during four seasons (winter: December to February; pre-monsoon: March to May; monsoon: June to September; and post-monsoon: October and November)~~Table 1 provide the details of the stations considered along with the total number of data available during different monsoon seasons (winter; December to February, pre-monsoon;; March to May, monsoon; June to September, and post-monsoon; October and November)~~. Fig. 2 shows the correlation coefficient along with the number of data points used in the analysis for the comparison between ~~the~~ estimated CAPE from the INSAT-3D measurements, ERA-Interim CAPE, and radiosonde derived CAPE. Here, the comparison is performed only when the INSAT-3D and radiosonde CAPE as well as INSAT-3D and ERA-Interim CAPE greater than zero. From this figure, it is noticed that the INSAT-3D estimated CAPE shows ~~the~~ better correlation with radiosonde CAPE compared to the ERA-Interim CAPE. In general, the coastal stations show a higher correlation coefficient than that of the other stations for the INSAT-3D estimated CAPE. All the coastal stations show a correlation higher than 0.6 except Trivandrum. The correlation coefficient is as high as 0.84 for Chennai among all the stations. The correlation values are lower for the stations located near the foothills of ~~the~~ Himalayas and north-east (NE) regions of India. A weak correlation of 0.31 is found for Delhi. For the ERA-Interim data, INSAT-3D CAPE shows less correlation coefficient for all the stations except Amini Divi compared to radiosonde CAPE~~The ERA-Interim estimated CAPE shows less correlation coefficient for all the stations except Agarthala compared to the INSAT-3D estimated CAPE~~. Even in the ERA-Interim CAPE, the coastal stations show better correlation compared to other stations. The ERA-Interim CAPE shows a higher correlation for Minicoy~~Agarthala~~ and the correlation is minimum for ~~Port Blair~~Delhi. This result suggests that the INSAT-3D CAPE measurements agree well with the radiosonde measurements. ~~It is worth to note that the comparison shows better correlation for the stations where the number of data is higher.~~

To elucidate the consistency of INSAT-3D estimated CAPE against the ERA-Interim CAPE, the bias in the measurements of INSAT-3D and ERA-Interim with the radiosonde is presented in Fig. 3. The bias evaluates the size of the difference between the two datasets. The positive (negative) value of bias indicates the overestimation (underestimation) of the satellite/reanalysis measurements. The INSAT-3D estimated CAPE shows small and positive bias for most of the stations considered in the study. Among all the stations, Hyderabad, Gorakhpur, and Delhi show higher bias, whereas Mumbai shows minimum bias. All the stations show positive bias except Ahmedabad, Dibrughar, Delhi, Gorakhpur, and Port Blair where the bias is negative and Mumbai shows small negative bias. Whereas, the ERA-Interim CAPE shows negative bias for all the stations indicating the underestimation of CAPE compared to radiosonde measurements. Further, the bias in the estimation of CAPE in the

ERA-Interim data is higher for most of the stations. Among all the stations, Gorakhpur shows higher negative bias. From this, it is clear that the INSAT-3D (ERA-Interim) overestimated (underestimated) the CAPE compared to radiosonde measurements. From the above discussion, it can be concluded that the INSAT-3D provides better estimates over coastal regions compared to other regions and also a better comparison with the radiosonde measurements.

4.2. *Statistical indices in the estimation of CAPE from~~in the comparison of~~ INSAT-3D ~~estimated CAPE~~measurements*

Furthermore, to examine the capability of detection of the INSAT-3D sounder, the probability of detection (POD), false alarm ratio (FAR), critical success index (CSI), and accuracy (ACC) are computed on the basis of a contingency table (Table ~~1~~2). A threshold value of zero is considered for CAPE to be estimated by the satellite measurements. The POD is a measure of the CAPE successfully identified by the satellite product, and FAR gives a proportional measure of the satellite product's tendency to estimate CAPE where none is observed i.e., it gives the CAPE estimates that are incorrectly detected. CSI represents how well the estimated CAPE events correspond to the observed CAPE events. ACC measures the fraction of the correctness in the CAPE estimates. For a perfect satellite-based estimate, the values of POD, FAR, CSI, and ACC should be 1, 0, 1, and 1 respectively. These statistical indices can be calculated as:

$$POD = \frac{a}{a+c} \qquad (2)$$

Formatted: Font: (Intl) Cambria Math

Formatted: Font: (Intl) Cambria Math

$$FAR = \frac{b}{a+b} \qquad (3)$$

Formatted: Font: (Intl) Cambria Math

Formatted: Font: (Intl) Cambria Math

$$CSI = \frac{a}{a+b+c} \quad (4)$$

$$ACC = \frac{a+d}{a+b+c+d} \quad (5)$$

Fig.~~ure~~ 4(a)-(d) shows the POD, FAR, CSI, and ACC calculated for the INSAT-3D estimated CAPE respectively. Among all the stations, Mumbai shows higher POD whereas Hyderabad shows lower POD. This indicates that the INSAT-3D is unable to detect CAPE over Hyderabad. This may be due to less availability of data and the inability to catch the short-lived convective storms frequently observed over this region. All the coastal stations show ~~the~~ higher POD, CSI, and ACC. Cochin shows the highest CSI and ACC, whereas Agarthala and Kolkata have highest FAR. This indicates that the INSAT-3D product performs reasonably well with the higher POD, CSI, and ACC and lower FAR.

4.3. *Distribution of CAPE over Indian Sub-continent*

A summary of the frequency distribution of CAPE computed from the INSAT-3D, ERA-Interim and radiosonde measurements for the 20 stations are shown in Fig.~~ure~~ 5. The distribution of CAPE shows ~~the~~ higher occurrence for lower values. Thus, the CAPE distribution is shifted to lower values in all the three measurements. The INSAT-3D estimated CAPE and ERA-Interim CAPE shows a similar kind of distribution compared to radiosonde CAPE. The distribution of the INSAT-3D estimated CAPE is higher (lower) in the range ~300-1200 (1200-3000) J kg^{-1} compared to the radiosonde measurements. The INSAT-3D estimated CAPE matches with the radiosonde CAPE above 3000 J kg^{-1}. The ERA-Interim CAPE distribution shows higher values below 1200 J kg^{-1}. However, the ERA-Interim distribution becomes negligible above 2000 J kg^{-1}. This also shows that for the higher values of CAPE, ~~the~~ ERA-Interim underestimates the observations. This may be due to the fact that the spatial resolution of the reanalysis data are coarse compared to the observations. The figure shows that among the two distributions, the INSAT-3D distribution agrees well with the radiosonde distribution.

4.4. *Seasonal variation of CAPE*

In the present study, the INSAT-3D dataset is dividedwe have divided the period into four seasons viz., winter (December to February), pre-monsoon (March to May), monsoon (June to September), and post-monsoon (October and November) to understand the seasonal variations in CAPE over the Indian region. Fig. 6(a)-(d) shows the seasonal mean CAPE estimated from the INSAT-3D measurements during the period from April-2014 to March-2017 over the Indian region. During the winter season (Fig. 6a), the mean CAPE is below 500 J kg^{-1} over the land regions. The mean CAPE is relatively higher over the west coast and Arabian Sea (AS) and the parts of northern Bay of Bengal (BoB). This relatively high CAPE over oceans and the western coastal regions may be due to the occurrence of depression and cyclone during the month of December over the oceanic regions. In the pre-monsoon season (Fig. 6b), the higher values of CAPE (above 2000 J kg^{-1}) are observed over the AS, BoB and Central India (CI). The pre-monsoon depressions are regular during this time period over the surrounding oceanic regions of India. This sustains for few days which results in higher CAPE over these regions. Higher values of CAPE are the causing factors for frequent thunderstorms and deep convection over the Northern and Central India. The Western Ghats has higher CAPE which may be due to the orographic induced deep convection. CAPE is lower over the Southern Peninsular India. Further, the CI, north India (NI) and foothills of Himalayas also exhibits higher CAPE compared to other land regions. The north-western parts of India (Gujarat) show higher CAPE among other land regions. During the monsoon season (Fig. 6c), the east coast of India, AS, BoB, and foothills of Himalayas shows relatively higher CAPE than the other regions. During the post-monsoon period (Fig. 6d), the northern parts of AS and BoB, east coast of India and west coast of India shows higher values of CAPE and the southern peninsula and eastern regions shows lower CAPE.

Further, the spatial distribution of CAPE estimated from the INSAT-3D is studied for different CAPE ranges. The spatial distribution of CAPE provides information on the distribution of extreme weather events over the study region. The estimated CAPE is divided into four categories: weak instability (<500 J kg^{-1}), moderate instability (501-1500 J kg^{-1}), strong instability (1501-3000 J kg^{-1}), and extreme instability (>3000 J kg^{-1}). The normalized anomaly distribution of CAPE in the four instability conditions during different seasons is provided over the Indian region as shown in Fig. 7. The spatial distribution of CAPE during the weak, moderate, strong, and extreme instability conditions is shown in Fig. 7(a)-(d), 7(e)-(h), 7(i)-(l), and 7(m)-(p) respectively. The top panel is for the winter, second from the top is for the pre-monsoon, third from the top is for the monsoon and bottom panel is for the post-monsoon season. Here, the negative (positive) anomaly indicates the increase (decrease) in CAPE. During ~~the~~ winter, the response of weak instability (Fig 7a) is very less over the Indian subcontinent as well as the surrounding oceanic regions. ~~-~~However, the response of winter towards strong and extreme instability is observed over the BoB, Southeast AS, and some parts of the NI. The higher response may be due to the cyclones and depressions that occur over the oceanic regions during December. Over the NI, strong westerlies are observed during the winter, which may result in a dry convection with higher CAPE.

The response during pre-monsoon is observed to be higher for ~~-during~~ strong and extreme instability. The pre-monsoon season is considered to be summer over the Indian subcontinent and it is the favorable season for thunderstorms and deep convection. This could be easily observed in the figure that during extreme instability the whole Indian region is observed to have higher frequencies ~~very high values~~ of CAPE. During ~~the~~ monsoon season, the response to weak and moderate instability is more compared to strong and extreme instability. It is observed that the Western Ghats and the surrounding oceanic regions have more frequency of weak and moderate instabilities compared to the other regions. The Western Ghats is generally dominated by the shallow clouds (e.g., Das et al., 2017; Utsav et al., 2017), which results ~~its~~ in high response with weak instability as deep convection does not predominantly occur over this region. The monsoon trough region extending from heat low in Pakistan to head BoB respond to strong instability. This trough (core low-pressure region) occurs during the monsoon, which results in heavy rainfall over the Indian subcontinent. Compared to the pre-monsoon, there is little response in strong instability conditions over the oceanic regions. This results in fewer occurrences of deep convection and cyclones (inhibited because of the presence of strong wind shear at 500 hPa) during the monsoon season. In the post-monsoon, the response is much similar to the pre-monsoon during the strong and extreme instability conditions. In ~~the~~ post-monsoon, the wind flow over the Indian region is northeasterly which results in more convection over the northwestern and the southern peninsular Indian region. Usually, in October-November months, the deep depression occurs over the Bay of Bengal due to which ~~the~~ higher frequency of ~~higher~~ CAPE is observed. In general, ~~the~~ weak instability is predominant during ~~the~~ winter season. The moderate instability shows higher occurrence during ~~the~~ post-monsoon compared to other seasons. The strong instability condition is more during the monsoon period whereas the occurrence of extreme instability is higher during ~~the~~ pre-monsoon months.

4.5. *Diurnal variation of CAPE*

Fig. 8 shows ~~the~~ hourly mean CAPE averaged for three years (2014-2017). A strong diurnal variation in the mean CAPE is observed over different parts of India. A clear land-sea contrast is also observed in the mean CAPE. The CAPE starts building up in the morning (0530 LT=00UTC+0530) over the oceans with land having low values of CAPE. The mean CAPE reaches its maximum at ~1200 LT over the oceans. However, the CAPE starts increasing after 0900 LT over the land and reaches the maximum in the afternoon (between 1300 and 1400 LT) and decreases again thereafter. The land-sea contrast in the mean CAPE has disappeared in the evening. Again in the evening, the CAPE increases and a secondary maximum is observed in the midnight over the oceans. Over the tropics, the Indian region is one of the active convective regions. The deep convective clouds form during the daytime over the Indian sub-continent due to solar insolation, which increases the lower tropospheric temperature resulting in convective instability. Uma and Das (2016) have found the lower tropospheric humidity maximum in the afternoon and minimum in the evening hours. The surrounding oceanic regions found to peak in the late evening and midnight. This indicates that the convection peaks in the late afternoon over the land region and evening to midnight over the oceans. These results are consistent with the findings of Dutta and Rao (2001) and Dutta and Kesarkar (2004). These studies revealed that the maximum value of CAPE is observed during nighttime over the BoB and east coast of India. However, this secondary maximum is not observed over the land areas. In contrast, another maximum is observed around 1700 LT over the east coast, west coast and north-west regions of India.

To observe the diurnal variation of CAPE over different parts of India, the study region is divided (latitude-wise for uniformity) into six sub-regions as provided in Raut et al. (2009). These regions are: the Arabian Sea (AS; 8-20^{o}N, 65-72^{o}E), Bay of Bengal (BoB; 8-20^{o}N, 80-90^{o}E), South Peninsular India (SP; 8-20^{o}N, 72-80^{o}E), Central India (CI; 20-25^{o}N, 73-82^{o}E), North India (NI; 25-35^{o}N, 73-80^{o}E), and Northeast India (NE; 24-29^{o}N, 90-96^{o}E). Fig. 9 shows the diurnal variation of mean CAPE over these sub-regions during four seasons. From this figure, one can observe a bimodal distribution in the mean CAPE over the AS and BoB during the pre-monsoon and monsoon periods (Fig. 9a and b). The primary maximum is observed in the nighttime and the secondary maximum is observed in the afternoon time over these regions. Uma and Das (2016) have also observed bimodal distribution in the relative humidity over the Bo~~Bay of Bengal~~ and the Indian Ocean. They found maximum distribution at 1200 and 1500 LT, which is almost similar to that observed in the present study. During Bay of Bengal Monsoon Experiment (BOBMEX) 1999, Dutta and Kesarkar (2004) observed that the CAPE is maximum in the nighttime than in the daytime. Further, the nighttime maximum in the mean CAPE is observed around ~0000 LT over BoB, and AS during the pre-monsoon and monsoon periods. The bimodal distribution in mean CAPE is also observed over the AS and BoB during ~~the~~ post-monsoon season. However, the secondary maximum is not much prominent as observed in the pre-monsoon and monsoon periods. The mean CAPE peaks in the afternoon hours over the AS and BoB during ~~the~~ winter season.

The SP region (Fig. 9c) also shows the similar behavior as that of oceans. The mean CAPE over the SP region maximizes in the afternoon hours. The secondary maximum is also observed in the late night (0000 LT). The mean CAPE in the CI region (Fig. 9d) shows a bimodal distribution during ~~the~~ winter, monsoon and post-monsoon seasons. The mean CAPE is at its maximum in the afternoon time. The other maximum is during the nighttime. A noticeable difference is observed in the mean CAPE during the pre-monsoon season. During this period, the CAPE is nearly the same throughout the day. However, this CAPE decreases a little and becomes minimum in the early morning over the CI region. The mean CAPE in the NI region (Fig. 9e) shows a similar diurnal variation as observed over the CI region. The mean CAPE shows little variation during the pre-monsoon months. The other three seasons show bimodal distribution as observed in other regions. However, the magnitude of the mean CAPE is higher in the NI region compared to the CI region. Further, the difference in mean CAPE between primary and secondary maximum is relatively small compared to the other regions. The NE region (Fig. 9f) also shows a bimodal distribution in mean CAPE with the primary maximum in the afternoon hours and the secondary maximum in the late-night during ~~the~~ winter, monsoon and post-monsoon seasons. In addition to these two maxima, a third maximum is also observed over the NE region during the pre-monsoon season. The third maximum is observed at ~0900 LT over this region. The third maximum observed in the mean CAPE may be due to the occurrence of pre-monsoon thunderstorms known as Norwesters during the morning over this region.

The statistical analysis of CAPE is also attempted over these six regions to understand the variability during different seasons ~~between the different regions~~as shown ~~during different seasons and it is shown~~ in Fig. 10~~(a)-(d) for the winter, pre-monsoon, monsoon, and post-monsoon respectively~~. The mean, standard deviation along with maximum/minimum with 25, 50 and 70 % occurrence are provided in the figure. During ~~the~~ winter, the mean CAPE is higher (~1600 J kg^{-1}) over the AS compared to that of the BoB (~1000 J kg^{-1}). Over the land regions, the mean CAPE is found to be less than ~1000 J kg^{-1}. The oceanic regions are found to have higher CAPE during ~~the~~ winter compared to that of the continent. The NI and NE have smaller CAPE during ~~the~~ winter period. W~~The w~~inter is extremely dry over the Indian region except for the surrounding oceanic regions and south peninsular India, where we observe cyclones/depressions during December, which brings more moisture and heavy rainfall as discussed earlier. During ~~the~~ pre-monsoon months, the mean CAPE is higher than ~2000 J kg^{-1} over all the regions concerned. The pre-monsoon depressions, thunderstorms, deep convection and Norwesters contribute to ~~very high~~higher CAPE values over India and surrounding oceanic regions. During ~~the~~ monsoon season, the mean CAPE is less than ~1500 J kg^{-1} over all the regions except the NI where it is about ~2000 J kg^{-1}. The shallow convection dominates during the monsoon season rather than deep convection, which results in ~~lesser~~ lower CAPE values compared to that of the pre-monsoon. During ~~the~~ post-monsoon, the mean value of CAPE is about ~1200 J kg^{-1} except AS where it is about ~1800 J kg^{-1} and BoB about ~1500 J kg^{-1}. The northeast monsoon dominates the Indian region during ~~the~~ post-monsoon which results in deep convection resulting in relatively higher values of CAPE. Overall, ~~over the Indian and the surrounding oceanic regions,~~ the maximum CAPE is found in the pre-monsoon followed by the post-monsoon, monsoon and winter over the Indian sub-continent.

5. Summary

The extreme weather events such as thunderstorms and tropical cyclones cause severe damage to life and property, especially in the tropical regions. Convective available potential energy (CAPE) is a measure of the amount of energy available for convection in the atmosphere. Hence, CAPE can be used as a measure for the occurrence of these severe weather conditions. In the present study, we made an attempt for the first time to estimate CAPE from the INSAT-3D measurements and evaluate comprehensively over the Indian ~~region~~sub-continent. For the evaluation, 20 stations are selected in different parts of India and these estimates are evaluated against the radiosonde measurements collected from the Wyoming University along with the ERA-Interim data. The station wise comparison shows that the INSAT-3D estimates match well with higher correlation coefficient and lower bias with the radiosonde measurements. The correlation coefficient between INSAT-3D and radiosonde CAPE is higher than that between INSAT-3D and ERA-Interim ~~and radiosonde~~. Further, the INSAT-3D derived CAPE overestimate the radiosonde CAPE ~~compared to radiosonde measurements~~, whereas the ERA-Interim ~~estimates~~ underestimate the radiosonde CAPE. The categorical statistics shows that the INSAT-3D can better represent the radiosonde measured CAPE. The distribution of CAPE ~~collected from all the 20 stations shows that the CAPE distribution~~ is ~~shifted to~~higher for lower values (< 1000 J kg^{-1}) in all the three ~~measurements~~datasets (radiosonde, INSAT-3D and ERA-Interim) for all the stations. The INSAT-3D and ERA-Interim estimated CAPE is higher than the radiosonde

Formatted: Not Highlight

Formatted: Not Highlight

Formatted: Superscript, Not Highlight

Formatted: Not Highlight

measurements in the lower ranges. The INSAT-3D estimated CAPE matches well with the radiosonde measurements above ~3000 J kg^{-1}.

The spatial and temporal distribution of CAPE reveals ~~several interesting features. The~~that the weak instability is predominant during ~~the~~ winter season, ~~the~~ moderate instability is higher during ~~the~~ post-monsoon, ~~the~~ strong instability is more during ~~the~~ monsoon period and ~~the~~ extreme instability is higher during ~~the~~ pre-monsoon months. The diurnal variation in mean CAPE shows a bimodal distribution with ~~the~~ primary peak around mid-night and secondary peak in the afternoon times for most of the regions and in different seasons. The seasonal mean CAPE shows that the land areas show lower CAPE during ~~the~~ winter, whereas the oceans show the highest CAPE during ~~the~~ pre-monsoon season. The higher values of CAPE over the oceanic regions may be due to ~~the higher sea surface temperature and~~ higher occurrence of the tropical cyclones during the pre-monsoon season. Further, the north-western parts of India ~~(Gujarat)~~ show higher CAPE among other land regions. Overall, the INSAT-3D estimated CAPE is in close agreement with the radiosonde derived CAPE. As the INSAT-3D provides high temporal and spatial resolution data, hence it can be used for now-casting and severe weather warnings in the numerical prediction models.

Acknowledgement

The authors sincerely acknowledge the Director, IITM for his constant support and encouragement during this study. The authors would like to acknowledge Meteorological and Oceanographic Satellite Data Archival Centre (MOSDAC) of Space Application Centre (~~ISRO~~SAC), ISRO for supplying the INSAT-3D data. The authors are grateful to the Department of Atmospheric Science, University of Wyoming for access to their radiosonde data archive. The authors acknowledge ~~the NOAA and~~ the ERA-Interim team for providing their data. All the dataset are freely available and can be downloaded from their respective archive. The authors would like to sincerely thank the Editor and two anonymous reviewers for ~~his~~ their insightful comments that improved the quality of the manuscript.

References:

Arakawa, A. and Schubert, W. H.: Interaction of a Cumulus Cloud Ensemble with the Large-Scale Environment, Part I, J. Atmos. Sci., 31(3), 674–701, doi:10.1175/1520-0469(1974)031<0674:IOACCE>2.0.CO;2, 1974.

~~Barnes, L. R., Gruntfest, E. C., Hayden, M. H., Schultz, D. M. and Benight, C.: False Alarms and Close Calls: A Conceptual Model of Warning Accuracy, Weather Forecast., 22(5), 1140–1147, doi:10.1175/WAF1031.1, 2007.~~

~~Bhat, G. S., Srinivasan, J. and Gadgil, S.: Tropical Deep Convection, Convective Available Potential Energy and Sea Surface Temperature, J. Meteorol. Soc. Japan. Ser. II, 74(2), 155–166, doi:10.2151/jmsj1965.74.2_155, 1996.~~

Bevington, P. R., Robinson, D. K.: Data reduction and Error Analysis for the Physical Sciences. McGraw-Hill, New York, 1992.

~~Botes, D., Mecikalski, J. R. and Jedlovec, G. J.: Atmospheric Infrared Sounder (AIRS) sounding evaluation and analysis of the pre-convective environment, J. Geophys. Res. Atmos., 117(D9), n/a–n/a, doi:10.1029/2011JD016996, 2012.~~

~~Breznitz, S.: The false alarm effect. Cry Wolf: The Psychology of False Alarms, Lawrence Erlbaum, 9–16, 1984.~~

Brooks, H. E.: Severe thunderstorms and climate change, Atmos. Res., 123(Supplement C), 129–138, doi:https://doi.org/10.1016/j.atmosres.2012.04.002, 2013.

~~Cintineo, J. L., Pavolonis, M. J., Sieglaff, J. M. and Lindsey, D. T.: An Empirical Model for Assessing the Severe Weather Potential of Developing Convection, Weather Forecast., 29(3), 639–653, doi:10.1175/WAF-D-13-00113.1, 2014.~~

Formatted: Font: Times New Roman, 12 pt

Formatted: Normal, Indent: Left: 0 cm, Hanging: 0.79 cm

~~Craven, J. P.: A preliminary look at deep layer shear and middle level lapse rates during major tornado outbreaks. Preprints, 20th Conf. on Severe Local Storms, Orlando, FL, *Amer. Meteor. Soc.*, 547-550, 2000.~~

Das, S. K., Konwar, M., Chakravarty, K. and Deshpande, S. M.: Raindrop size distribution of different cloud types over the Western Ghats using simultaneous measurements from Micro-Rain Radar and disdrometer, Atmos. Res., 186, 72–82, doi:http://dx.doi.org/10.1016/j.atmosres.2016.11.003, 2017.

de Coning, E., Koenig, M. and Olivier, J.: The combined instability index: A new very-short range convection forecasting technique for southern Africa, Meteorol. Appl., 18(4), 421–439, doi:10.1002/met.234, 2011.

Dee, D. P., Uppala, S. M., Simmons, A. J., Berrisford, P., Poli, P., Kobayashi, S., Andrae, U., Balmaseda, M. A., Balsamo, G., Bauer, P., Bechtold, P., Beljaars, A. C. M., van de Berg, L., Bidlot, J., Bormann, N., Delsol, C., Dragani, R., Fuentes, M., Geer, A. J., Haimberger, L., Healy, S. B., Hersbach, H., Hólm, E. V, Isaksen, L., Kållberg, P., Köhler, M., Matricardi, M., McNally, A. P., Monge-Sanz, B. M., Morcrette, J.-J., Park, B.-K., Peubey, C., de Rosnay, P., Tavolato, C., Thépaut, J.-N. and Vitart, F.: The ERA-Interim reanalysis: configuration and performance of the data assimilation system, Q. J. R. Meteorol. Soc., 137(656), 553–597, doi:10.1002/qj.828, 2011.

DeMott, C. A. and Randall, D. A.: Observed variations of tropical convective available potential energy, J. Geophys. Res. Atmos., 109(D2), n/a–n/a, doi:10.1029/2003JD003784, 2004.

Dhaka, S. K., Sapra, R., Panwar, V., Goel, A., Bhatnagar, R., Kaur, M., Mandal, T. K., Jain, A. R. and Chun, H.-Y.: Influence of large-scale variations in convective available potential energy (CAPE) and solar cycle over temperature in the tropopause region at Delhi (28.3°N, 77.1°E), Kolkata (22.3°N, 88.2°E), Cochin (10°N, 77°E), and

Trivandrum (8.5°N, 77.0°E) using radiosonde during 1980–2005, Earth, Planets Sp., 62(3), 319–331, doi:10.5047/eps.2009.09.001, 2010.

Donner, L. J. and Phillips, V. T.: Boundary layer control on convective available potential energy: Implications for cumulus parameterization, J. Geophys. Res. Atmos., 108(D22), n/a–n/a, doi:10.1029/2003JD003773, 2003.

~~Doswell, C. A.: Weather Forecasting by Humans—Heuristics and Decision Making, Weather Forecast., 19(6), 1115–1126, doi:10.1175/WAF-821.1, 2004.~~

Dutta, S. N., and Kesarkar, A.P.: Diurnal and spatial variation of convective parameters over Bay of Bengal during BOBMEX 1999, *2*(April), 323–328, 2004.

Dutta, S. N., and Rao, G.S.P.: Diurnal and spatial variation of stability parameters at coastal stations along the East Coast, during BOBMEX- 1999 , Proceedings of the TROPMET 2001 Symposium, 336-346, 2001.

~~Dutta, S. N., and De, U.S.: A diagnostic study of contrasting rainfall epochs over Mumbai, Mausam, (February 1998), 1-8, 1999.~~

Gaffen, D. J., Barnett, T. P. and Elliott, W. P.: Space and Time Scales of Global Tropospheric Moisture, J. Clim., 4(10), 989–1008, doi:10.1175/1520-0442(1991)004<0989:SATSOG>2.0.CO;2, 1991.

Gartzke, J., Knuteson, R., Przybyl, G., Ackerman, S. and Revercomb, H.: Comparison of Satellite-, Model-, and Radiosonde-Derived Convective Available Potential Energy in the Southern Great Plains Region. *J. Appl. Meteor. Climatol.*, **56**, 1499–1513, https://doi.org/10.1175/JAMC-D-16-0267.1, 2017.

Gettelman, A., Seidel, D. J., Wheeler, M. C. and Ross, R. J.: Multidecadal trends in tropical convective available potential energy, J. Geophys. Res. Atmos., 107(D21), ACL 17–1–ACL 17–8, doi:10.1029/2001JD001082, 2002.

Formatted: Font: Times New Roman, 12 pt

Formatted: Normal, Indent: Left: 0 cm, Hanging: 1 cm

~~Golden, J. H., and Adams, C.R.: The Tornado Poblem: Forecast, Warning, and Response, Nat. Hazards Review, 1 (2), 107-118, 2000.~~

Jewett, C. P. and Mecikalski, J. R.: Estimating convective momentum fluxes using geostationary satellite data, J. Geophys. Res. Atmos., 115(14), 1–13, doi:10.1029/2009JD012919, 2010.

Johns, R. H. and Doswell, C. A.: Severe Local Storms Forecasting, Weather Forecast., 7(4), 588–612, doi:10.1175/1520-0434(1992)007<0588:SLSF>2.0.CO;2, 1992.

Koenig, M. and de Coning, E.: The MSG Global Instability Indices Product and Its Use as a Nowcasting Tool, Weather Forecast., 24(1), 272–285, doi:10.1175/2008WAF2222141.1, 2009.

Lee, M.-I., Schubert, S. D., Suarez, M. J., Held, I. M., Kumar, A., Bell, T. L., Schemm, J.-K. E., Lau, N.-C., Ploshay, J. J., Kim, H.-K. and Yoo, S.-H.: Sensitivity to Horizontal Resolution in the AGCM Simulations of Warm Season Diurnal Cycle of Precipitation over the United States and Northern Mexico, J. Clim., 20(9), 1862–1881, doi:10.1175/JCLI4090.1, 2007.

~~McNulty, R. P.: Severe and Convective Weather: A Central Region Forecasting Challenge, Weather Forecast., 10(2), 187–202, doi:10.1175/1520-0434(1995)010<0187:SACWAC>2.0.CO;2, 1995.~~

Mitra, A. K., Bhan, S. C., Sharma, A. K., Kaushik, N., Parihar, S., Mahandru, R. and Kundu, P. K.: INSAT-3D vertical profile retrievals at IMDPS , New Delhi : A preliminary evaluation operational High resolution Infrared Radiation Sounder, 4(October), 687–694, 2015.

Moncrieff, M. W. and Miller, M. J.: The dynamics and simulation of tropical cumulonimbus and squall lines, Q. J. R. Meteorol. Soc., 102(432), 373–394, doi:10.1002/qj.49710243208, 1976.

Murugavel, P., Pawar, S. D. and Gopalakrishnan, V.: Trends of Convective Available Potential Energy over the Indian region and its effect on rainfall, Int. J. Climatol., 32(9), 1362–1372, doi:10.1002/joc.2359, 2012.

Narendra Babu, A., Nee, J. B. and Kumar, K. K.: Seasonal and diurnal variation of convective available potential energy (CAPE) using COSMIC/FORMOSAT-3 observations over the tropics, J. Geophys. Res. Atmos., 115(D4), n/a–n/a, doi:10.1029/2009JD012535, 2010.

Ratnam, M. V., Hemanth Kumar, A. and Jayaraman, A.: Validation of INSAT-3D sounder data with in situ measurements and other similar satellite observations over India, Atmos. Meas. Tech., 9(12), 5735–5745, doi:10.5194/amt-9-5735-2016, 2016.

Raut, B. A., Karekar, R. N., and Puranik, D. M.: Spatial distribution and diurnal variation of cumuliform clouds during Indian Summer Monsoon. J. Geophys. Res. Atmos., 114(11), 1–12. https://doi.org/10.1029/2008JD011153, 2009.

Riemann-Campe, K., Fraedrich, K. and Lunkeit, F.: Global climatology of Convective Available Potential Energy (CAPE) and Convective Inhibition (CIN) in ERA-40 reanalysis, Atmos. Res., 93(1), 534–545, doi:https://doi.org/10.1016/j.atmosres.2008.09.037, 2009.

~~Rothfusz, L. P., Karstens, C. and Hilderband, D.: Next-Generation Severe Weather Forecasting and Communication, Eos, Trans. Am. Geophys. Union, 95(36), 325–326, doi:10.1002/2014EO360001, 2014.~~Santhi, Y. D., Ratnam, M. V., Dhaka, S. K., and Rao, S. V.: Global morphology of convection indices observed using COSMIC GPS RO satellite measurements. Atmos. Res., 137, 205–215. https://doi.org/10.1016/j.atmosres.2013.10.002, 2014.

Field Code Changed

Formatted: No underline, Font color: Auto

Formatted: No underline, Font color: Auto

Field Code Changed

Siewert, C. W., Koenig, M. and Mecikalski, J. R.: Application of Meteosat second generation data towards improving the nowcasting of convective initiation, Meteorol. Appl., 17(4), 442–451, doi:10.1002/met.176, 2010.

Uma, K. N. and Das, S. K.: Do the stability indices indicate the formation of deep convection?, Meteorol. Atmos. Phys., doi:10.1007/s00703-017-0550-9, 2017.

Uma, K. N. and Das, S. S.: Quantitative and qualitative assessment of diurnal variability in tropospheric humidity using SAPHIR on-board Megha-Tropiques, J. Atmos. Solar-Terrestrial Phys., 146(Supplement C), 89–100, doi:https://doi.org/10.1016/j.jastp.2016.05.009, 2016.

Utsav, B., Deshpande, S. M., Das, S. K. and Pandithurai, G.: Statistical Characteristics of Convective Clouds over the Western Ghats Derived from Weather Radar Observations, J. Geophys. Res. Atmos., 122(18), 10,10–50,76, doi:10.1002/2016JD026183, 2017.

Washington, W. M. and Parkinson, C. L.: Introduction to three-dimensional climate modeling, University Science Books,Mill Valley, CA, United States, 2005. [online] Available from: http://www.osti.gov/scitech/servlets/purl/7120862, 1986.

Williams, E., Rosenfeld, D., Madden, N., Gerlach, J., Gears, N., Atkinson, L., Dunnemann, N., Frostrom, G., Antonio, M., Biazon, B., Camargo, R., Franca, H., Gomes, A., Lima, M., Machado, R., Manhaes, S., Nachtigall, L., Piva, H., Quintiliano, W., Machado, L., Artaxo, P., Roberts, G., Renno, N., Blakeslee, R., Bailey, J., Boccippio, D., Betts, A., Wolff, D., Roy, B., Halverson, J., Rickenbach, T., Fuentes, J. and Avelino, E.: Contrasting convective regimes over the Amazon: Implications for cloud electrification, J. Geophys. Res. Atmos., 107(D20), LBA 50-1-LBA 50-19, doi:10.1029/2001JD000380, 2002.

~~Williams, E. and Renno, N.: An Analysis of the Conditional Instability of the Tropical Atmosphere, Mon. Weather Rev., 121(1), 21–36, doi:10.1175/1520-0493(1993)121<0021:AAOTCI>2.0.CO;2, 1993.~~

Table Captions:

Table 1: The total number of data available during four ~~monsoon~~ seasons for the 20 stations for the period from April~~,~~ 2014 to March~~,~~ 2017.

Table ~~1~~2: Contingency table for the comparison of INSAT-3D estimated CAPE with radiosonde measured CAPE. The CAPE threshold is ~~assumed~~ considered as 0 J kg^{-1}.

Figure Captions:

Fig 1: The geographical map of India representing the 20 stations considered for the present study. ~~Stations are Agarthala (AGR; 23.88˚N, 91.25˚E); Ahmedabad (AHB; 23.06˚N, 72.63˚E); Amini Divi (AMD; 11.12˚N, 72.73˚E); Bhuvaneswar (BHU; 20.25˚N, 85.83˚E); Chennai (CHE; 13.00˚N, 80.18˚E); Cochin (COC; 9.95˚N; 76.26˚E); Delhi (DEL; 28.58˚N, 77.20˚E); Dibrugarh (DIB; 27.48˚N, 95.01˚E); Gorakhpur (GRK; 26.75˚N, 83.36˚E); Guwahati (GUW; 26.10˚N; 91.58˚E); Hyderabad (HYD; 17.45˚N, 78.46˚E); Karaikal (KAR; 10.91˚N, 79.83˚E); Kolkata (KOL; 22.65˚N, 88.45˚E); Machilipatnam (MAP; 16.20˚N, 81.15˚E); Mangalore (MAN; 12.95˚N, 74.83˚E); Minicoy (MIN; 8.30˚N, 73.15˚E); Mumbai (MUM; 19.11˚N, 72.85˚E); Port Blair (PB; 11.66˚N, 92.71˚E); Trivandrum (TVM; 8.48˚N, 76.95˚E); Visakhapatnam (VSP; 17.70˚N, 83.30˚E).~~

Fig 2: (a) Correlation ~~Coefficient~~ coefficient in the comparison of INSAT-3D ~~and ERA~~ CAPE with radiosonde and ERA-Interim~~derived~~ CAPE for 20 stations in India for the ~~Period~~ period April~~,~~ 2014 to March~~,~~ 2017. **(b)** Number of data points in the comparison of INSAT-3D~~-~~ CAPE~~, ERA-CAPE~~ with radiosonde and ERA-Interim CAPE.

Fig 3: Bias in the comparison between INSAT-3D~~-~~ CAPE and ERA-Interim reanalysis CAPE with radiosonde for different ~~Stations~~ stations in India for the ~~Period~~ period April~~,~~ 2014 – March~~,~~ 2017.

Fig 4: Statistical indices (a) POD, (b) FAR, (c) CSI and (d) ACC in the comparison between the INSAT-3D~~-~~ CAPE with radiosonde CAPE for 20 ~~Stations~~ stations in India.

Fig 5: Distribution (%) of INSAT-3D, radiosonde and ERA-Interim reanalysis CAPE (J kg^{-1}) for all the stations considered in the study.

Fig. 6: The ~~seasonal mean~~ distribution of CAPE (J kg^{-1}) during (a) winter (b) pre-monsoon (c) monsoon and (d) post-monsoon from INSAT-3D data over Indian region.

Fig. 7: Frequency distribution (%) of CAPE in (a) weak (b) moderate (c) strong (d) extreme instability during winter season. (e)-(h): same as (a)-(d) except for pre-monsoon season. (i)-(l): same as (a)-(d) but for monsoon season and (m)-(p): same as (a)-(d) except for post-monsoon season.

Fig 8: Hourly mean distribution of ~~the~~ INSAT-3D CAPE (J kg^{-1}) during the period from 01 April 2014 to 31 March 2017 over the Indian region.

Fig 9: Diurnal variation of CAPE (J kg^{-1}) over (a) AS (b) BoB (c) SP (d) CI (e) NI (f) NE region of India during four ~~monsoon~~ seasons.

Fig 10: Box-plot analysis ~~of distribution~~ of CAPE (J kg^{-1}) during (a) winter (b) pre-monsoon (c) monsoon and (d) post-monsoon from INSAT-3D data over six sub-regions over the Indian sub-continent. ~~the Indian region.~~

Table 1: The total number of data available during four ~~monsoon~~ seasons for the 20 stations for the period from April~~,~~ 2014 to March~~,~~ 2017.

Station	Latitude	Longitude	Total Number of Data			
			Winter	**Pre-monsoon**	**Monsoon**	**Post-monsoon**
Agarthala (AGR)	23.88	91.25	3614	3272	2615	2613
Ahmedabad (AHB)	23.06	72.63	3808	4034	3686	2891
Amini Divi (AMD)	11.12	72.73	3985	3776	3327	2362
Bhuvaneswar (BHU)	20.25	85.83	3701	3450	2389	2488
Chennai (CHE)	13.00	80.18	3816	3712	2956	1985
Cochin (COC)	9.95	76.26	3867	3072	2905	1758
Delhi (DEL)	28.58	77.20	2910	3316	3845	2894
Dibrugarh (DIB)	27.48	95.01	3287	2260	2536	2595
Gorakhpur (GRK)	26.75	83.36	2871	3383	2769	2833
Guwahati (GUW)	26.10	91.58	3610	3058	2956	2796
Hyderabad (HYD)	17.45	78.46	2550	394	327	1045
Karaikal (KAR)	10.91	79.83	3660	3458	3632	1846
Kolkata (KOL)	22.65	88.45	3488	2924	2500	2677
Machilipatnam (MAP)	16.20	81.15	4001	3706	2564	2322
Mangalore (MAN)	12.95	74.83	4063	3542	2705	2232
Minicoy (MIN)	8.30	73.15	3882	3346	3320	2040

Mumbai (MUM)	19.11	72.85	4294	4321	3405	2756
Port Blair (PB)	11.66	92.71	3676	3458	2381	2178
Trivandrum (TVM)	8.48	76.95	3675	3116	3608	1805
Visakhapatnam (VSP)	17.70	83.30	3972	3747	2632	2415

Table ~~1~~2: Contingency table for the comparison of INSAT-3D estimated CAPE with radiosonde measured CAPE. The CAPE threshold is ~~assumed~~ considered as 0 J kg^{-1}.

	Radiosonde ≥Threshold	Radiosonde < Threshold
Satellite ≥Threshold	Hits (a)	False alarms (b)
Satellite <Threshold	Misses (c)	Correct negatives (d)

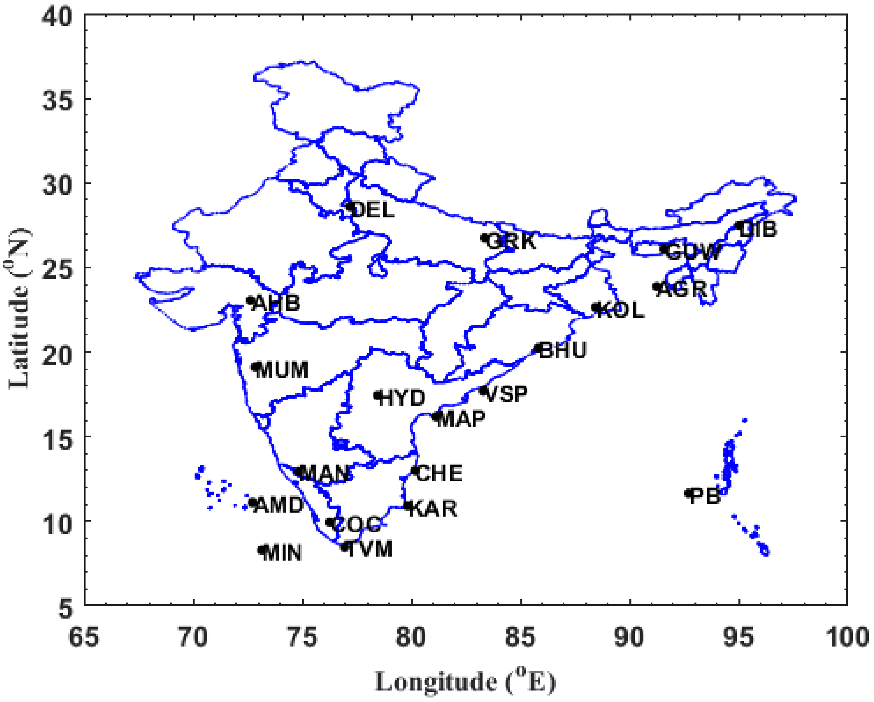

Fig 1: The geographical map of India representing the 20 stations considered for the present study. Stations are Agarthala (AGR; 23.88˚N, 91.25˚E); Ahmedabad (AHB; 23.06˚N, 72.63˚E); Amini Divi (AMD; 11.12˚N, 72.73˚E); Bhuvaneswar (BHU; 20.25˚N, 85.83˚E); Chennai (CHE; 13.00˚N, 80.18˚E); Cochin (COC; 9.95˚N; 76.26˚E); Delhi (DEL; 28.58˚N, 77.20˚E); Dibrugarh (DIB; 27.48˚N, 95.01˚E); Gorakhpur (GRK; 26.75˚N, 83.36˚E); Guwahati (GUW; 26.10˚N; 91.58˚E); Hyderabad (HYD; 17.45˚N, 78.46˚E); Karaikal (KAR; 10.91˚N, 79.83˚E); Kolkata (KOL; 22.65˚N, 88.45˚E); Machilipatnam (MAP; 16.20˚N, 81.15˚E); Mangalore (MAN; 12.95˚N, 74.83˚E); Minicoy (MIN; 8.30˚N, 73.15˚E); Mumbai (MUM; 19.11˚N, 72.85˚E); Port Blair (PB; 11.66˚N, 92.71˚E); Trivandrum (TVM; 8.48˚N, 76.95˚E); Visakhapatnam (VSP; 17.70˚N, 83.30˚E).

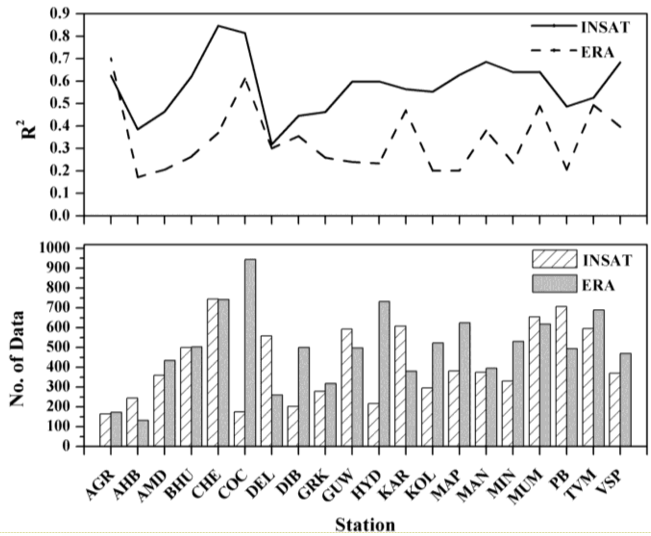

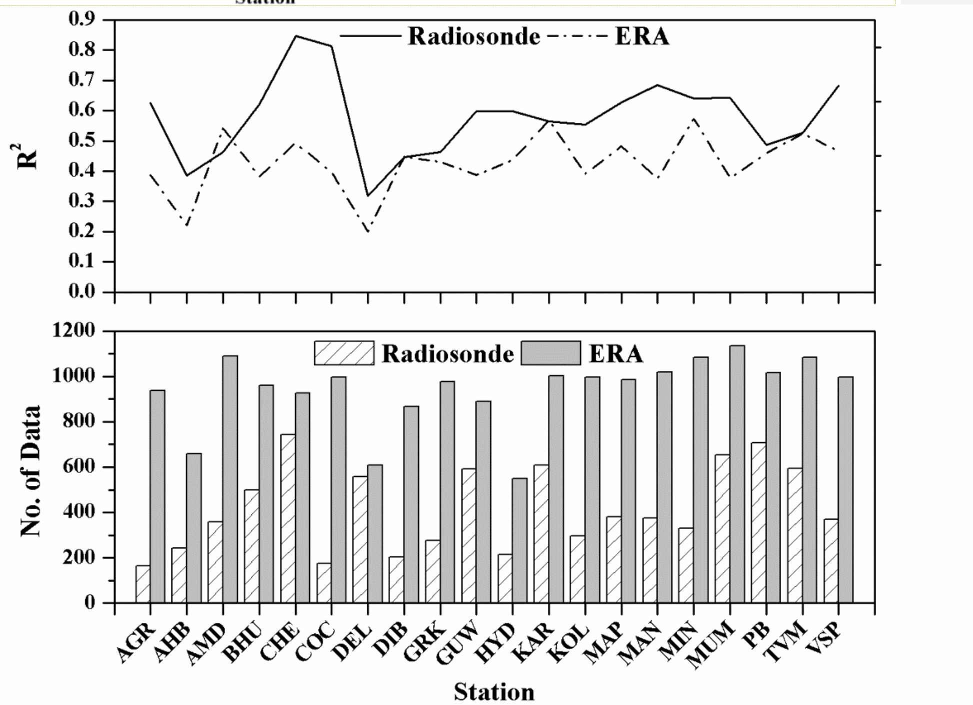

Fig 2: (a) Correlation coefficient in the comparison of INSAT-3D CAPE with radiosonde and ERA-Interim CAPE~~Correlation Coefficient coefficient in the comparison of INSAT-3D and ERA CAPE with radiosonde derived CAPE~~ for 20 stations in India for the ~~Period~~ period April~~,~~ 2014 to March~~,~~ 2017. **(b)** Number of data points in the

Formatted: Font: Times New Roman, 12 pt comparison of INSAT-3D~~-~~_CAPE~~, ERA-CAPE~~ with radiosonde and ERA-Interim CAPE.

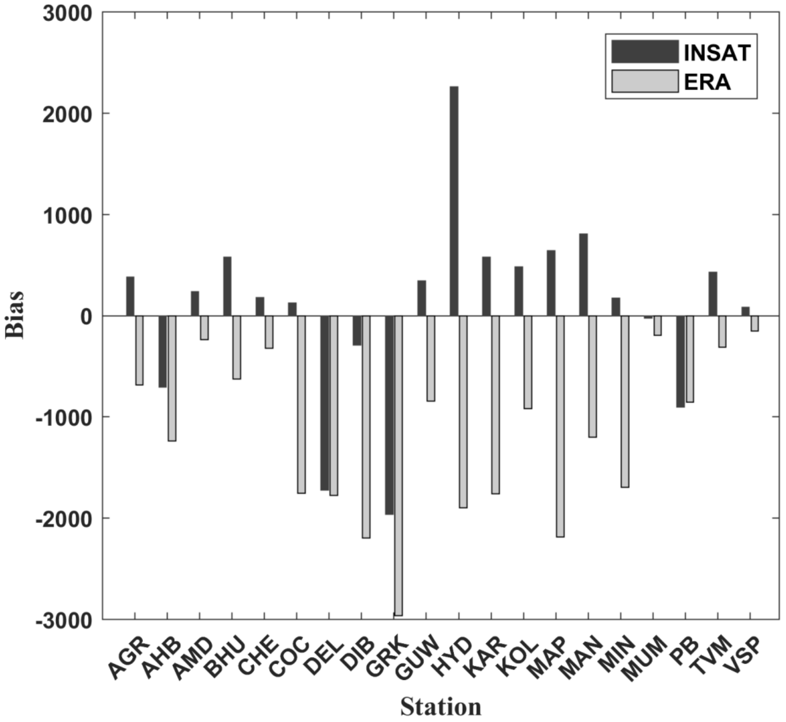

Fig 3: Bias in the comparison between INSAT-3D~~-~~_CAPE and ERA-Interim reanalysis CAPE with radiosonde for different Stations in India for the ~~Period~~ period April~~,~~ 2014 – March~~,~~ 2017.

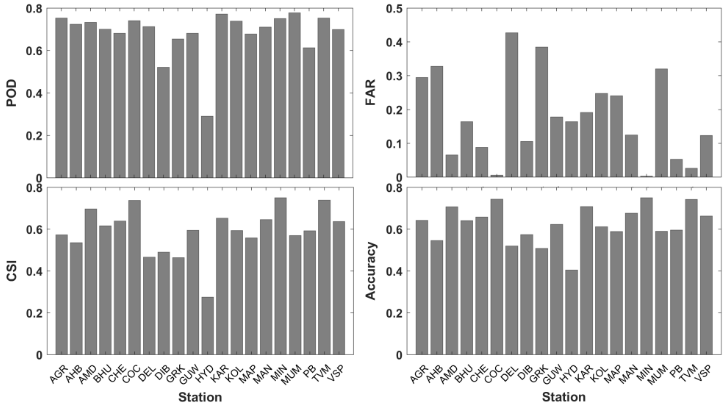

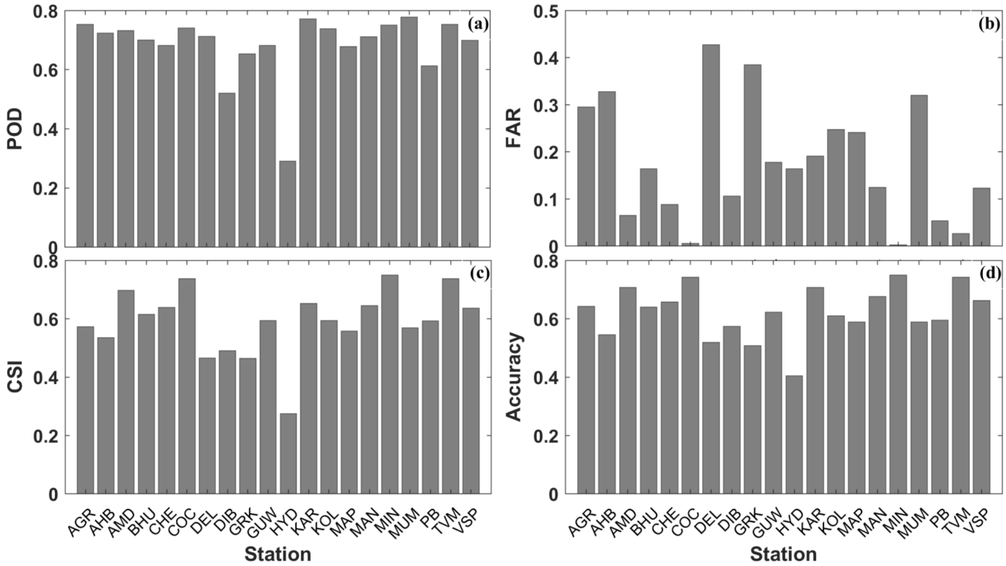

Fig 4: Statistical indices (a) POD, (b) FAR, (c) CSI and (d) ACC in the comparison between the INSAT-3D- CAPE with radiosonde CAPE for 20 ~~Stations~~ stations in India.

Formatted: Font: Times New Roman, 12 pt

Formatted: Centered

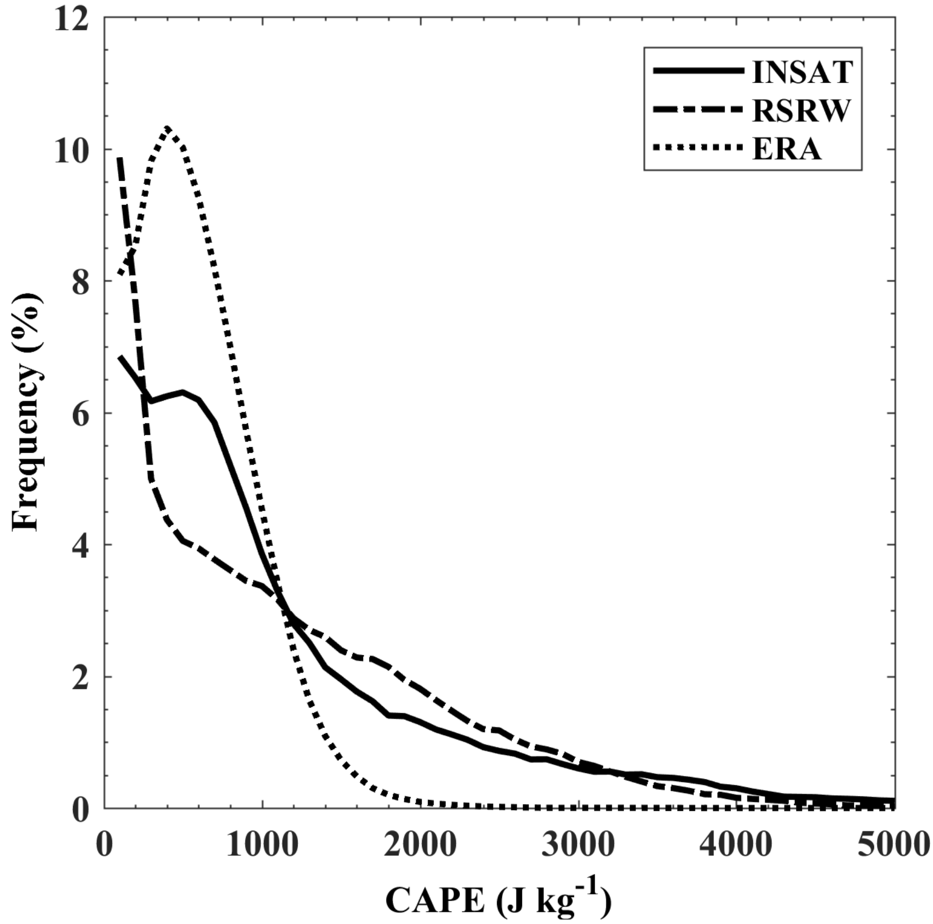

Fig 5: Distribution (%) of INSAT-3D, radiosonde and ERA-Interim reanalysis CAPE (J kg^{-1}) for all the stations considered in the study.

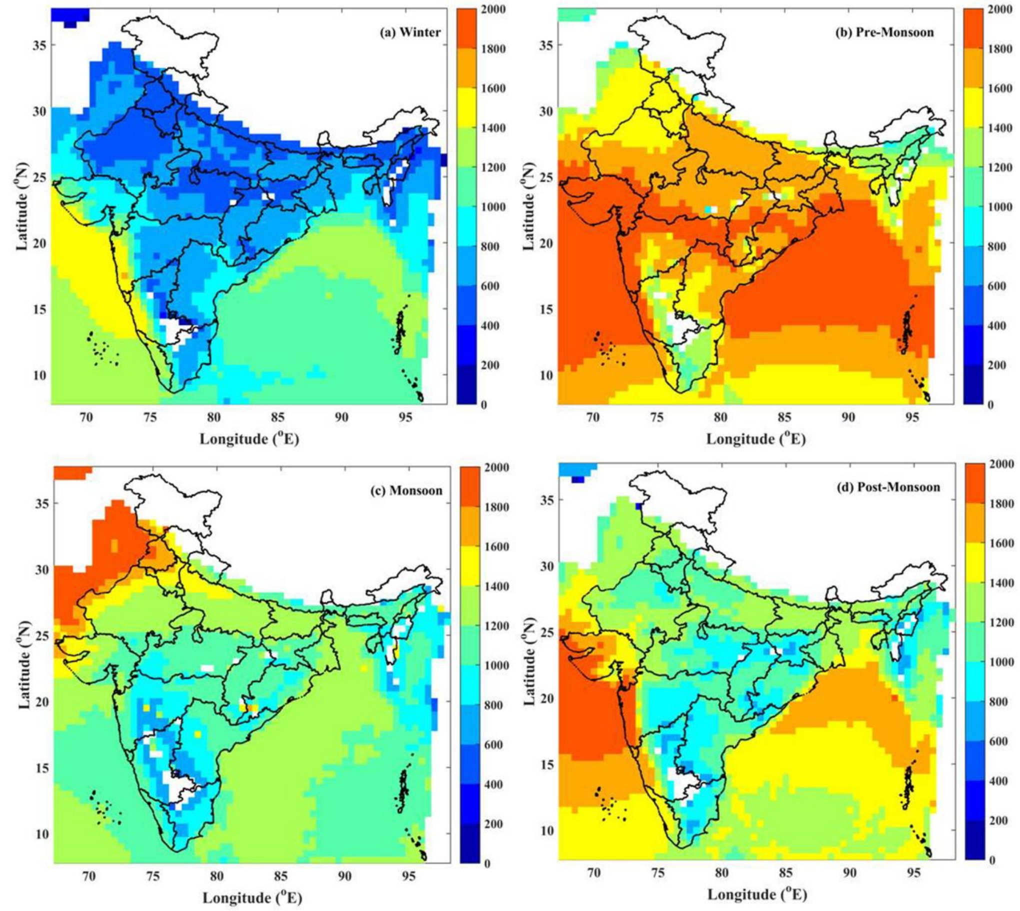

Fig. 6: The ~~seasonal mean~~ distribution of CAPE (J kg^{-1}) during (a) winter (b) pre-monsoon (c) monsoon and (d) post-monsoon from INSAT-3D data over Indian region.

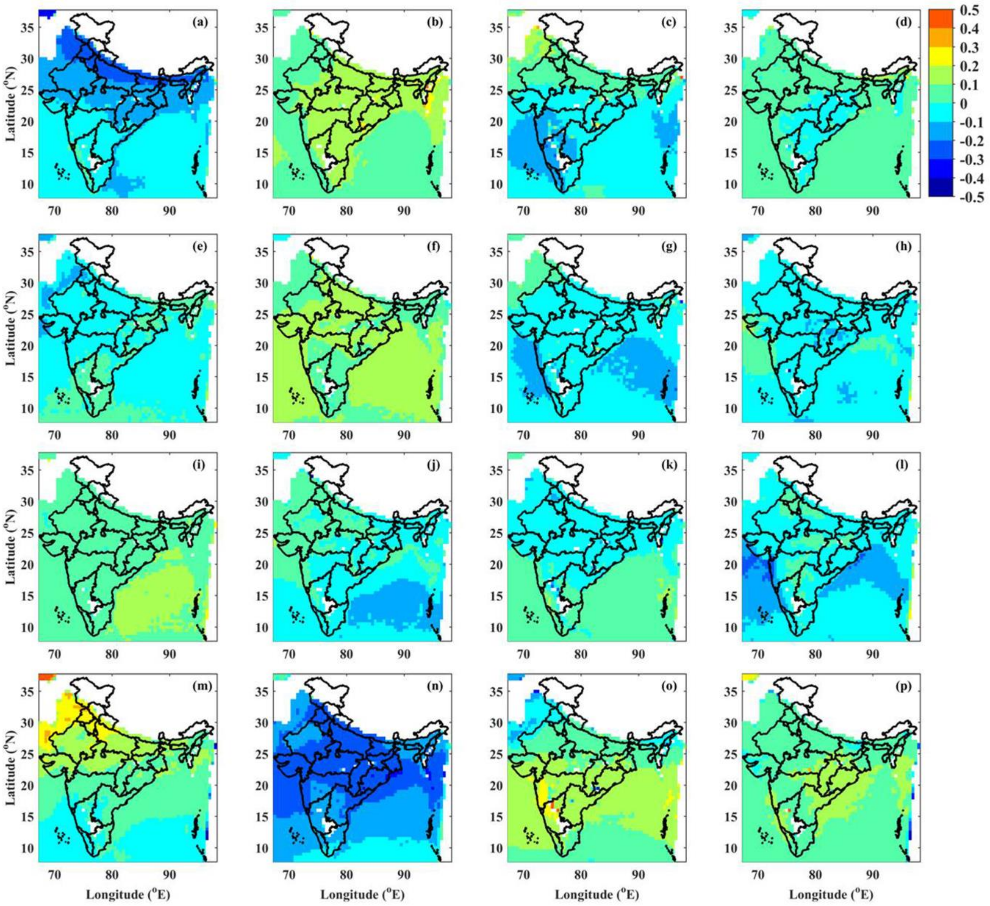

Fig. 7: Frequency distribution (%) of CAPE in (a) weak (b) moderate (c) strong (d) extreme instability during winter season. (e)-(h): same as (a)-(d) except for pre-monsoon season. (i)-(l): same as (a)-(d) but for monsoon season and (m)-(p): same as (a)-(d) except for post-monsoon season.

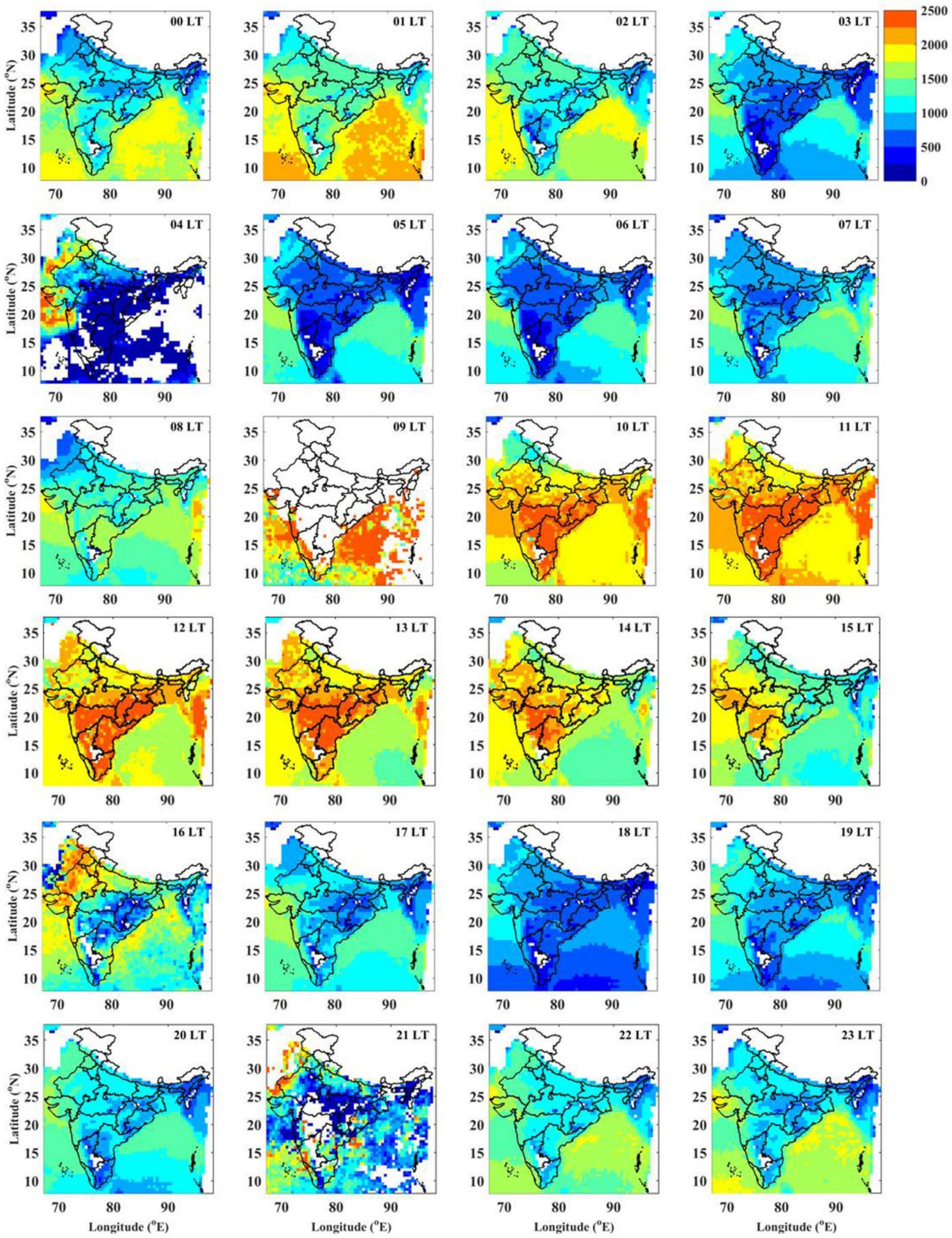

Fig 8: Hourly mean distribution of ~~the~~ INSAT-3D CAPE (J kg^{-1}) during the period from 01 April 2014 to 31 March 2017 over the Indian region.

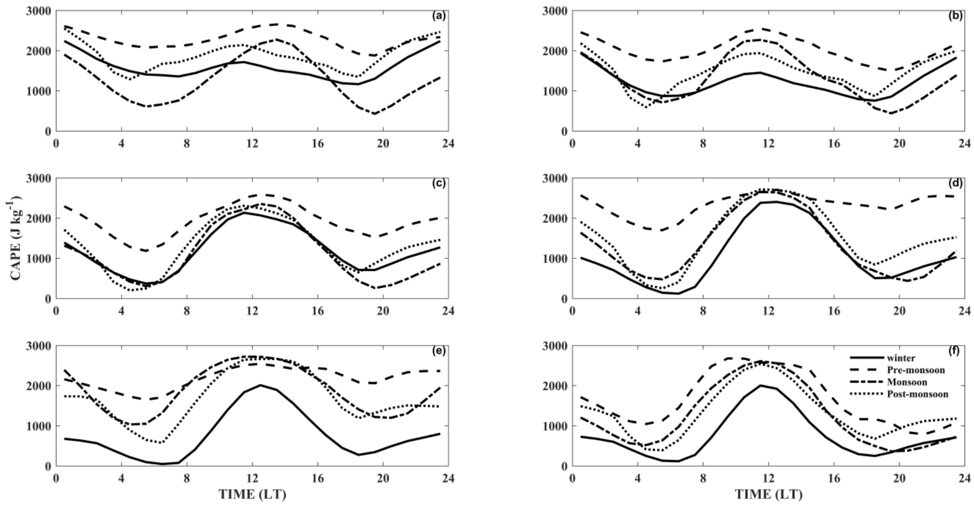

Fig 9: Diurnal variation of CAPE (J kg^{-1}) over (a) AS (b) BoB (c) SP (d) CI (e) NI (f) NE region of India during four ~~monsoon~~ seasons.

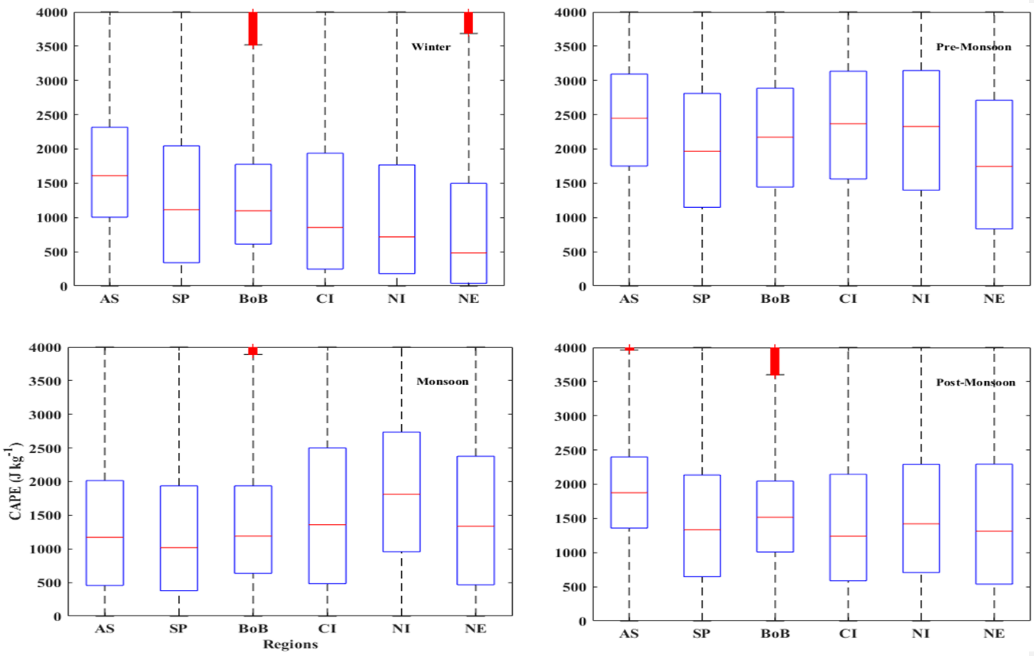

Fig 10: Box-plot analysis ~~of distribution~~ of CAPE (J kg^{-1}) during (a) winter (b) pre-monsoon (c) monsoon and (d) post-monsoon from INSAT-3D data over six sub-regions over the Indian sub-continent~~the Indian region~~.